PERFORMANCE PREDICTIONS OF PACKED BED LIQUID DESICCANT DE-HUMIDIFICATION SYSTEM OPERATING WITH NOVEL DESICCANT MIXTURES

*A thesis submitted in partial fulfilment of the requirement
for the degree of*

MASTER OF SCIENCE BY RESEARCH

By

Mahesh Mahajan

(Roll. No. 204351007)

Under the guidance of

Prof. P. Muthukumar

**School of Energy Science and Engineering
Indian Institute of Technology Guwahati
Guwahati -781039, India
August 2021**

CERTIFICATE

It is certified that the work contained in the progress report entitled **"Performance predictions of packed bed liquid desiccant de-humidification system operating with novel Desiccant mixtures"** submitted by **Mahesh Mahajan, Roll No. 204351007,** has been carried out under my supervision and that this work has not been submitted elsewhere for any degree.

Date:

Prof. P. Muthukumar

School of Energy Science and Engineering

Indian Institute of Technology, Guwahati

Guwahati-781039

ACKNOWLEDGEMENT

ABSTRACT

Growing Economies with growing per capita income has led to increase in the demand of more refrigeration systems. Most of refrigeration systems are energy intensive due to usage of VCR system and it is expected that on an average loss of 30% in refrigerant occurs throughout life cycle of the system and these emissions has negative impact on environment. Total energy consumption in the buildings due to refrigeration amounts to 20% which is high. India is signatory of the Kigali Agreement which focuses on the refrigerants and to reduce their usage. Therefore, we need to look after the new solution for the refrigeration air and conditioning system. The major energy consumption in air conditioning happens due to latent load. Hence we have to look after better solutions to it and most effective and promising solution these days seems to be the LDAC system.

Common Refrigeration system involves the dehumidification process which is highly energy consuming process and can be operated on low grade energy such as the solar and geothermal energy. Most promising amongst all is the solar energy. Here I have tried to use the solar energy a low grade energy to be utilized in a cycle with the help of liquid desiccant. Desiccants are the materials which has affinity to absorb the moisture present in air, by utilizing this property we can achieve the goal of dehumidification. When moisture is absorbed in the desiccant the heat of condensation is liberated and this increases the temperature of the absorbing medium and hence we need to reduce the desiccant solution temperature to its normal such that it can be operated in further cycles. For this purpose, we use the regenerator which in combination with the external air removes the moisture from the solution and decreases the temperature of the solution which can be operated again in cycle.

In subsequent chapters I have done an in depth literature survey from which I have tried to make a model which will help us to predict the performance of the dehumidifier for given input. From literature review I got to know that the most useful method is finite difference method and here I have tried to make a Numerical model for dehumidification system with that method.

To operate the LDAC system we need to pump the liquid and blow the air. This air which is when blown in the dehumidifier system where the packing material is structured for dehumidification

create an obstruction to the air movement. This obstruction creates pressure drop in the dehumidifier which ultimately adds to the blower energy costs. For better performance this pressure drop has to be reduced and hence a model is prepared to study the pressure drop in the dehumidifier packed bed structure.

Along with this model I have tried to see the various mass and heat transfer coefficient which govern the heat and mass transfer equations in the FDM model. This equation which are developed over the experimental data by various researchers vary greatly and hence a proper equations need to be selected for heat and mass transfer governing equations.

This study will help to make a model for the novel desiccant mixture which will be utilized for the prediction of performance of that desiccant with different structured packing.

SYMBOLS AND ABBREVIATIONS

Symbols

a_t	Total Specific surface area (m^2/m^3)
b	Corrugation base dimension, m
C	Specific heat capacity(kJ/kg.k)
D_p	Equivalent diameter, m
d_L	Diameter of the falling liquid particles(m)
D	Diffusivity (m^2/s)
F	F type mass transfer coefficient (kmole/m^2.s)
G	Air flow rate (kg/m^2.s)
g	Acceleration due to Gravity (m/s^2)
h	Corrugation crimp height, m
h	Volumetric heat transfer coefficient (kW/K.m^3)
h_a	Enthalpy of air (kJ/kg.K)
h_a	Static liquid holdup
L	Liquid Flow rate (kg/m^2.s)
K	Mass transfer coefficient (kmole/m^2.s.Pa)

m^*	Heat capacity ratio
M	Molar mass (kmole/kg)
P	Pressure (Pa)
S	Side dimension of corrugation (m)
R	Ideal gas constant(kJ/kmole.K)
Re	Reynolds number
Fr	Froude number
We	Weber number
Sc	Smidth number
Pr	Prandtl number
NTU	Number of Transfer Units
V	Volume (m^3)
u	Velocity (m/s)
T	Temperature in (℃)
X	Flooding coefficient
x_{SM}	Interfacial concentration
x	Concentration in Fraction of weight
Y	Specific humidity (kg/kg of dry air)

z   Element height(m)

Greek Symbol

ϵ Void Fraction

ε Effectiveness

β   Angle of inclined corrugation to the horizontal, (Degree)

σ Density (kg/m^3)

u Dynamic viscosity (Pa.s)

Ω   Packing surface void fraction

σ Surface tension (N/m)

ρ Density (kg/m^3)

Subscripts

L   Liquid

G   Gas

C   Critical

t   Total

sat   Saturation

v	Vapor
a	Air
p	Pressure
°	Reference state
e, p	Effective
ope	Operating
dry	Dry
tot	Total
in	Inlet
out	Outlet
r	Relative

CONTENT

LIST OF FIGURES

LIST OF TABLES

CHAPTER-1

INTRODUCTION

Energy is an essential pillar for the growth of every civilization; therefore, it's our prime duty to use energy efficiently and make continuous improvements in the energy consuming processes. One of the most energy intensive sector is refrigeration and air conditioning (RAC). Even in global pandemic of COWID 2019 the RAC industry has reported positive growth. In India, Room AC sales demand has shown positive growth since 2006 to 2017 where the demand was increased from the 2 million units to 30 million units [1].This increase in demand, is because of India's growth in per capita income. RAC is essential and is must in all walks of life such as health; but while discussing about health we have to consider the health of the environment as well. RAC mostly operate on the VCR system and it uses the high global warming potential refrigerants such as R134A, R410a, R404A [2][3]. India is the signatory of the Kigali agreement, in which we are supposed to reduce the use of environment degrading refrigerants [4]. It's prime time to look for

alternative solution for the VCR system which is high grade energy consuming process and to look for a system which is more environment friendly and can operate on the low grade energy, without compromising the reliability and effectiveness [5].

1.1 Refrigeration and Air Conditioning

Refrigeration is the general term which includes Heating, Ventilating and air conditioning; used to provide the necessary application oriented environment in controlled fashion. Air conditioning includes humidifying, dehumidifying, heating, cooling, filtering and distribution of air at suitable conditions to maintain human comfort or as per particular applications requirement. Refrigeration is important when it comes to storage of the goods, human environment and its comfort as in hospitals which require the fresh air in large quantity for operation theaters and in space shuttles and so on, the application of Heating, Ventilating and air conditioning are enormous and it is used in wide areas as well. Simple VCR cycle works on the bell Coleman cycle and it's the simplest cycle.

1.2 Why we need the LDAC over VCR

VCR system basically uses the compressor, condenser, capillary tube and produces the required conditions while working on the reverse bell Coleman cycle. The conventional VCR system has problem of not able to handle the latent load much effectively though it accounts for majority of the work and hence causing the oversizing of the system to handle the moisture. Dehumidification with VCR air conditioners by cooling air below its dew point to remove moisture and then reheating air to the desired delivery conditions and main load is due to latent heat only [6] [7] [8]. This problem can be reduced by using other system which works with the usage of low-grade energy such as waste heat or solar energy in accordance with the usage of desiccants. In below shown table we can see the pros and cons of the VCR and LDAC system [6]. Conventional VCR system if handling high value of latent heat can lead to the inefficient dehumidification process. An oversizing of the system adds an extra Burdon of the cost .In addition to above problems another problem is that when re-evaporation occurs in the building of the condensed moisture when the coil is off, this causes to decreases the efficiency of the system ,whenever system is switched on/off [7].

Table 1.1 Comparison between VCR and LDAC

Sr. No.	Parameter	VCR	LDAC
1	Indoor air quality	Average	High
2	Energy Source	Electrical or based on natural gas	Solar, Geothermal, Waste, low grade heat
3	Humidity Control	Average	Accurate
4	Operational Cost	High	Saves-40-50%
5	Energy Storage capacity	Low	High
6	Fluid	HFC, CFC, HCFC	LiCl, LiBr, $CaCl_2$, TEG, ZnBr
7	Environmental impact	Harmful	Comparatively eco friendly
8	System Installation	Average	Slightly Complicated

1.3 Desiccant Based Dehumidification

The desiccants are used for cooling and dehumidification of air to the required condition and can be operated by utilizing low grade heat, such as Solar energy and geothermal energy [8][9]. Desiccant air conditioning system work basically, by transferring the moisture from one airstream to another by using two processes. These processes are shown in the below figure;

- Sorption process
- Desorption process

1.3.1 Sorption Process

Difference between the vapor pressure of water vapor, between the solution and the air creates the potential for the mass transfer. If the desiccant solution material is concentrated and cold, so it has low vapor pressure and hence it absorbs the moisture from the air which has high vapor pressure of water vapor. In this process the latent heat is released and taken by the solution, and in response the air temperature may increase or decrease and the desiccant solution temp increases and it becomes less concentrated.
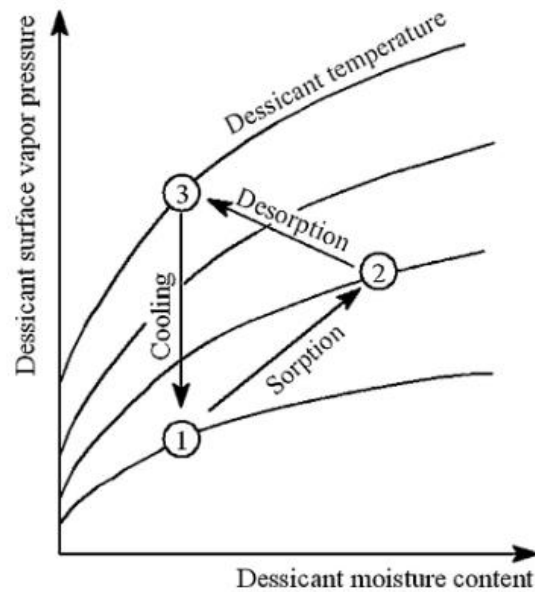
Figure 1.1 Process for transfer of moisture in desiccant system [10]

1.3.2 Desorption Process

The process of releasing the moisture captured by the desiccant solution to the air by increasing the temperature of the desiccant, also known as the process of regeneration. During this process we supply the thermal energy and this thermal energy increases the temperature of the desiccant solution ultimately creating the potential for mass transfer between the air and the solution. Here we can use basically the low-grade energy and this is what makes this technology more environmentally friendly compared to other technologies. The air which has lower temperature and lower vapor pressure than the surface vapor pressure of the diluted heated solution absorbs the moisture from the solution creating concentrated solution.

1.4 Dehumidification based on the type of the Desiccant

There are mainly 2 types of the systems based on the type of desiccant used and those are;

- Solid Desiccant System
- Liquid Desiccant system
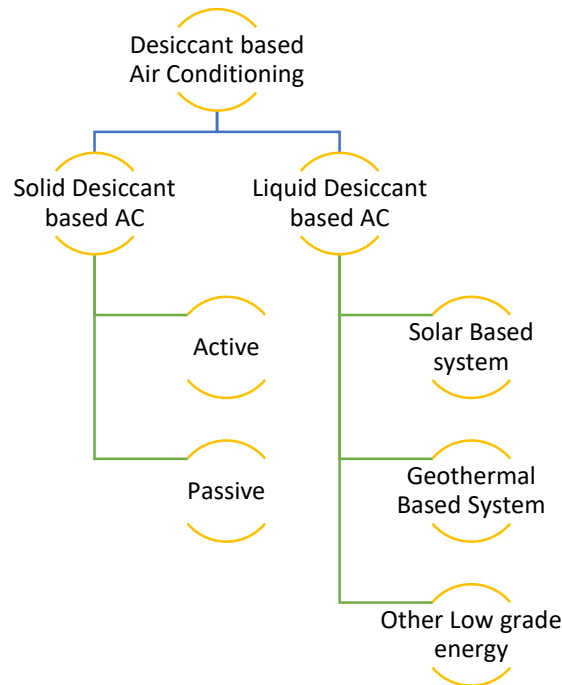
Figure 1.2 Types of Desiccant based Dehumidification systems

1.4.1 Solid Desiccant based Dehumidification

Solid desiccant-based system can be categorized based on the energy characteristics as active desiccant wheel and passive desiccant wheels.

1.4.1.1 Active Desiccant Wheel

It consists of a rotating drum fitted with a honeycomb packing. The desiccant coated walls act as a moisture absorbing spots when air is made to flow through it removes moisture from the air. The desiccant material continues the moisture uptake until half or three-quarters of the period of revolution. The regeneration is achieved by using hot air, by using the low-grade energy such as solar and geothermal energy.

1.4.1.2 Passive Desiccant Wheel

Passive wheel, also known as the enthalpy wheel use the exhaust air from the conditioned space. the enthalpy recovery wheel is placed between the fresh and exhaust streams, allowing the later to precool and dry the former. It typically rotates much faster (10–20 rpm) than a desiccant wheel (0.15–0.20 rpm). An important difference is that the regeneration is carried out by cold air, allowing for a reduced dehumidifying capacity when compared to an active desiccant wheel. A

comparative study revealed that the enthalpy recovery in passive desiccant wheels is as much as twice as in heat wheels.
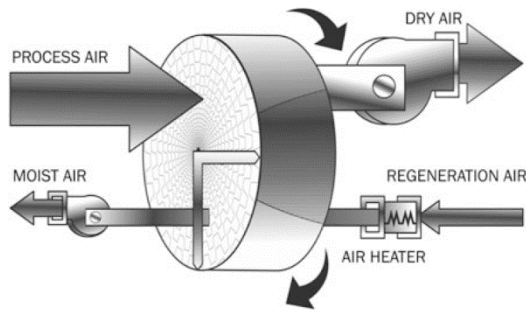
Figure 1.3 Active desiccant wheel
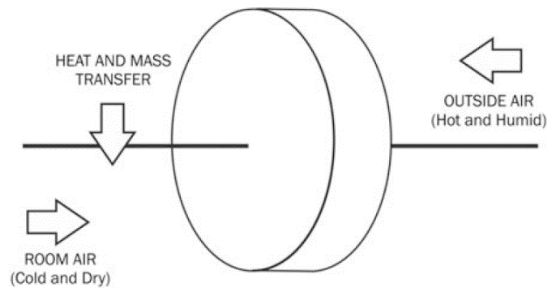
Figure 1.4 Passive Desiccant wheel

1.4.2 Liquid Desiccant based Refrigeration

A desiccant is a material that has a strong affinity for water (Adsorbs or Absorbs). It is common to classify desiccants as either solid or liquid depending on their normal physical state (although a material such as lithium chloride can be both, absorbing water vapor both as a solid, hydrated salt or as an aqueous solution). The strength of a desiccant can be measured by its equilibrium vapor pressure, i.e. pressure of water vapor that is in equilibrium with the desiccant. This equilibrium vapor pressure increases roughly exponentially with the temperature of the desiccant/water system. It also increases as the desiccant absorbs water, i.e., a dilute liquid desiccant will have a higher equilibrium vapor pressure than a concentrated liquid desiccant. When air flows over a surface that is wetted with a liquid desiccant, the desiccant can either absorb or desorb water depending on whether the desiccant's 'equilibrium' relative humidity is above or below the air's relative humidity. If the desiccant absorbs water from the air, heat will be released and the desiccant's temperature will increase. This heating is the inverse of evaporative cooling. By analogy to evaporative cooling, one can define a brine-bulb temperature as the temperature that the desiccant–air interface approaches. The brine-bulb temperature is a function of a liquid desiccant's concentration and the air's temperature and humidity.
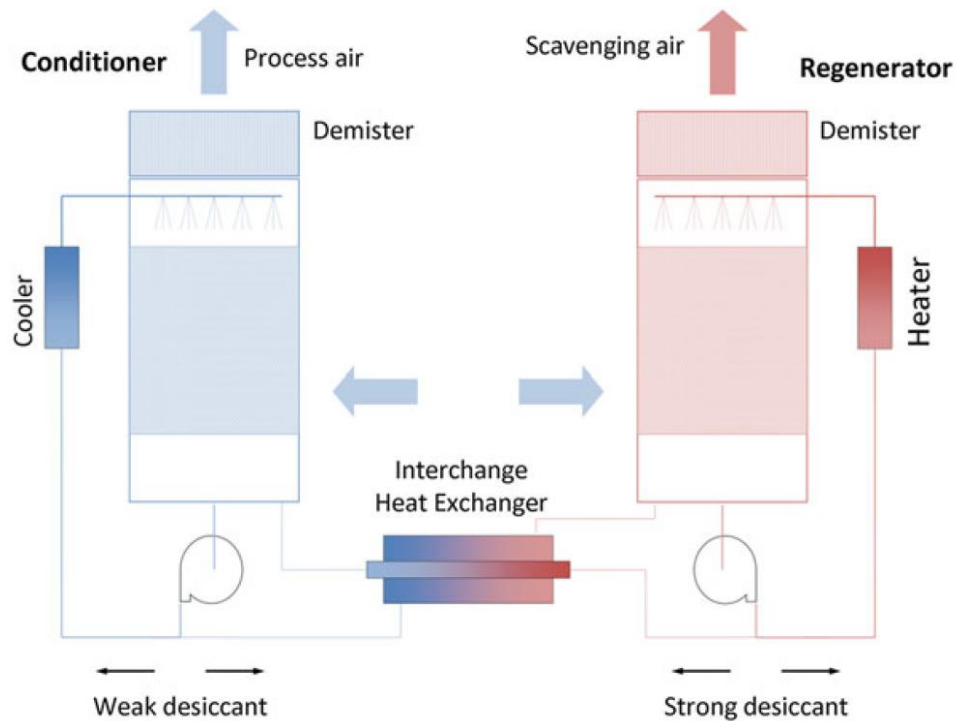
Figure 1.5 Liquid Desiccant System

The typical operation of a LDAC system is shown in above figure. The conditioner (also commonly called an absorber) is the component that cools and dries the process air. As shown in this figure, the conditioner is a bed of structured contact media, similar to the corrugated fill that might be used in a cooling tower. Liquid desiccant is first cooled in a heat exchanger and then sprayed onto the contact media. The desiccant flow rate must be sufficiently high to insure complete wetting of the media (i.e., about 5 g/min per square foot of face area [3.4 l/s. m2]). The process air gets cooled as when it come in contact with the structured mesh of ABS material and its temperature decreases as the moisture condense. Heat is released as the desiccant absorbs water from the air, but the high flow rate of desiccant limits its temperature rises to a few degrees. The regenerator removes the water that the desiccant has absorbed in the conditioner. The desiccant is regenerated by first heating it to raise its equilibrium vapor pressure. The hot desiccant, typically between 71.1 ^{0}C) and 93.3 ^{0}C, is sprayed over the structured mesh of ABS. Flow rate of desiccant is sufficiently high to insure complete wetting of the media. This hot desiccant is then made to have contact with air which is brought from outside and its temperature is less as the desiccant desorbs the water vapor to it. This air which has higher moisture content is exhausted to the ambient.

1.5 Types of Desiccant Material

Desiccant material absorbs the moisture present in the air when it is made to have contact with the air. Desiccant materials are basically hygroscopic in nature and they attract water vapor. Desiccant materials can be classified accordingly into liquid and solid type.

1.5.1 Liquid Desiccant Materials

The liquid desiccant when used, it not only absorbs the moisture present in the air but also heat can be removed simultaneously while heating and cooling process. The desired properties of the desiccant material are shown in below figure;

Table 1.2 Properties of Desiccant [11]

Absorption Properties	Transport properties	Economic and Enviremental properties
• Equivalent specific humidity • Enthalpy release while absobing moisture • Coefficient of Diffusuion • Enrgy Storage capacity	• Specific heat capacity • Viscosity • Density • Thermal conductivity • Surface tension	• Cost • Safety • Material Compatability

Basically, this system has the components like heat exchanger, regenerator, and dehumidifier sometimes dehumidifier and regenerator are referred to as conditioner[12].The material of desiccant does affect the design of the system and hence need to choose properly. Following qualities are need to found in desiccant [13],

- Low Initial Cost
- Low Operating Cost
- low Viscosity
- Stability
- Availability
- Rate of mass transfer should be high
- Non-Hazardous
- Low Flammability
- Low Surface Tension

- Low Corrosivity
- Easy to Maintain
- Low Heat of Adsorption

The real challenge is to find a desiccant which has all properties and in reality, no such material exists and hence we need to compromise between the available desired properties which a desiccant exhibit. Most of the popular desiccants has some of the above properties, but not all of them.

Table 1.3 Comparison of Liquid and Solid Dehumidification technique [14]

Sr. No	Parameter	Liquid Desiccant dehumidification	Solid desiccant dehumidification
1	volatile organic compounds	Removal	Removal
2	Bacteria	Kill or deactivation	No effect
3	Particular Matters	Capture	Release
4	Carryover	Yes	No

1.5.2 Solid Desiccant Materials

Solid desiccant materials are one of the first tested materials for achieving the moisture absorbing capacity. Silica gel was used by the many researchers and still, to this date it is being used as the most abundantly for absorbing moisture, by keeping sachets of the silica gels inside the bags where moisture has to be absorbed by physio-sorption.

Ha et al., [15] used silica gel, which have the A,B types which differ in their adsorbent temperature, capacity and regenerative temperature. Carbon also acts as an adsorbent material as stated by the ha et al.

Hybrid mixture of the CaCl2 and silica gel B was used by **Tokarev et al**., [16] in their studies and it too showed great results compared to the alone action of the silica gel.

Metal–organic frameworks (MOFs)are of great importance because of their structure and desorbing temperature and can be used in many areas such as catalysis, gas storage. The cage like structure helps in achieving this edge over other desiccant materials[17]. There are some dies like Dry coconut coir which have also shown some results [18].

1.6 Objective of the Study

- To develop a finite difference model to predict the performance of the packed bed counter flow dehumidifier with LiCl desiccant solution.

- To develop a numerical model, to predict the pressure drop in packed bed counter flow dehumidifier with LiCl desiccant solution by varying packing density.

- To conduct experimental study on dehumidifier/ regenerator using binary desiccant mixture and optimize packing material for 0.5 TR cooling capacity at Indian Institute of Technology, Guwahati.

Chapter-2

LITERATURE SURVEY

Predicting the output of the system based on the given input has always been the challenge. Every time a new theory has been proposed brings a new dimension to the system study and same applies to the dehumidifier system as well.

2.1 Dehumidification Process

Dehumidification is a process which involves removal of moisture from the air. This can be achieved by the adsorption and absorption. The change in concentration of a given substance at the interface as compared with the neighboring phases is referred to as adsorption. Adsorption is a surface phenomenon and which adsorbs the moisture by utilizing the wander walls weak cohesive forces or hydrogen bonding in between the molecules, and this process is called the physio-sorption [19]. The case where the valence forces comes into account in dehumidification, can be

called as the chemisorption [20]. Dehumidification is energy intensive process which is used in air conditioning and can be operated with the help renewables such as solar and geothermal energy [8] [9]. Using solar energy for liquid desiccant system is not a new technology but it has become feasible in recent year due to recent developments in the solar energy field.

Basic major components of the desiccant system are the regenerator and dehumidifier. For liquid desiccant system the configuration varies for regenerator or dehumidifier as both components are quite similar in construction. There are basically three variations in the configuration as follows,

1. Spray Chamber
2. Packed Tower
3. Spray Coil

2.2 Heat Exchanger Packing

Y.J. Dai et al., [21] in their Numerical simulation and theoretical analysis with lithium chloride solution has shown that honeycomb packed tower configuration has given them good results and they found out the Nusselt number for the both liquid and air side and hence concluded that the given configuration is more suitable for the given application. Coefficient of heat transfer differ for the liquid and gas side because of the mixing heat generated in the dehumidification heats the air as well as the desiccant solution. Structured packing is preferred because of many reasons and we can compare the both random packing and structured packing conditioners as follows[12][22]. The humidifiers can be classified into further types as classified on the basis of its operation and structure as shown in the following flow diagram,

Table 2.1 Comparison of the Structured Packing Vs Random Packing

Sr. No.	parameter	Structured Packing	Random Packing
1	Structure	Uniform	Disturbed
2	Cost	Costlier	Cheaper
3	Pressure	Lesser air side pressure drop	Higher pressure drop due to irregular shape
4	Area	High	Lesser
5	transportation	Difficult to transport without damage	Easy to transport and storage
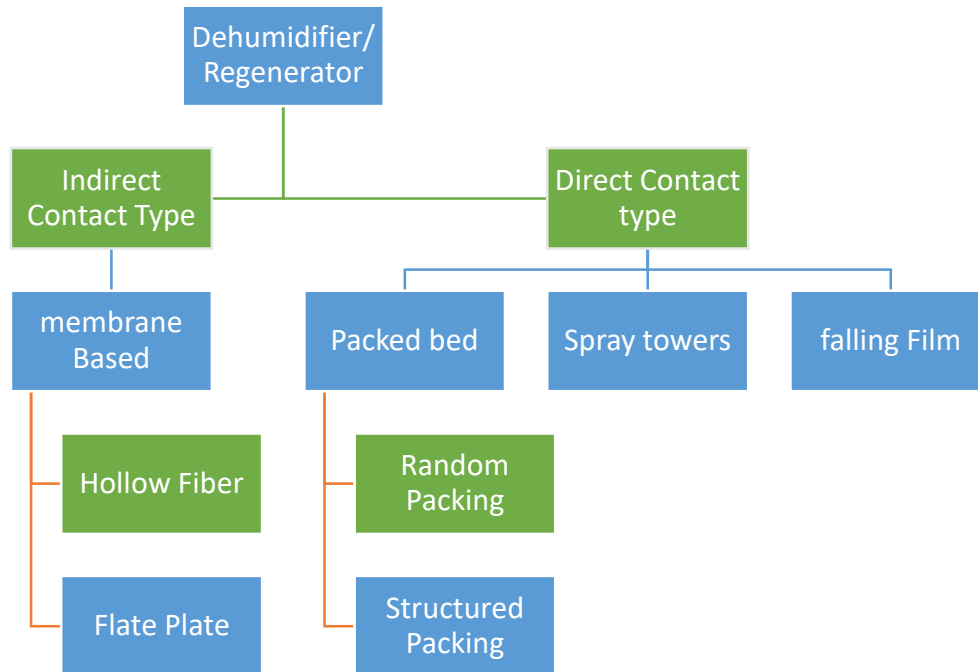
Figure 2.1 Classification of Dehumidifier or Regenerator [16]

2.2.1 Different types of the Packing Materials

Packing materials greatly affect the output of the dehumidifier. The channel through which the fluid flows and the place where heat and mass exchange take place depend on the packing material. The surface roughness and surface liquid film formation and most important effective diameter of the channel depend upon the packing [23]. Hence it is necessary to choose wisely the packing according to the requirement, as effective diameter depend upon the specific surface area and the void faction of the packing and packing geometry [24]. Again the packing has a great influence on the air side and liquid side heat and mass transfer coefficients [25].Mass transfer coefficients are the most important parameters which govern the humidity and temperature equations of dehumidifier [26].

Kaibal et al., [27] in their paper has studies the effect of using Montz packing manufactured by the Montz company. This packing is metallic and available in the standard angle of the 45^0 and 60^0 and has high specific area which can be made available from the 250 -750 m^2/m$^{3.}$ In this study they reproduced the results for the given packed Montz structure and found that the packing has reliable operation as per stated values in the catalogue. They used Delft model to produce and study the results and concluded that the CFD study with Fluent of 1phase fluid also has shown the

same results and the more in depth study of the 2 phase flow is yet in testing phase . Problem with this packing is its high cost and metallic nature as the solution of desiccant will corrode the packing, making it vulnerable for long run use and introducing impurities in the solution which directly will affect the solution vapor pressure [28].

Stichlmair et al., [29] has shown in his paper that total pressure drop with packing of Gempak 2A (having $\varepsilon=0.93$ $a_t=262$ m^2/m^3) increases with the liquid holdup.This packing is one of the suitable candidates for the dehumidifier packing because of standard availability of the packing made from non-corrosive materials.

Saeed et al., [30] conducted a simulation study with FLUENT and verified with experimental results on the Gempak 2A and found a relation for the effective area which participates in actual heat and mass transfer. The relation given extends on the relation given by the Conde et al., [31] for the LiCl and is valid for most of the desiccants.

Udara Arachchige, [31] in his paper has shown that the structured packing's has shown better performance compared to the Raschig rings. He has compared the effect of the packing material with the BX, Mellapak 350Y, Raschig rings. In his study researcher has shown that structured packing has better absorption characteristics compared to the 25mm Raschig packing. In random packing study Udara Arachchige found that Pall rings (size 16, 25, 38 mm) has shown better performance than the Raschig rings and has shown better performance characteristics for Pall rings of 16 mm size.

J. R. Ortiz-Del Castillo et al., [32] in his numerical and experimental study on counter flow packed bed system has shown that the performance of the Sulzer BX is better as it can be seen from the absorption percentages when compared to the pall rings.

Goswami et al., [26] in their work has used the Hi-flow polypropylene packing with 210 m^2/m^3. They used the counter-flow packed bed system to predict the performance of the dehumidifier system with LiCl desiccant solution. In this paper they gave equations for the performance prediction of the dehumidifier system along with effective area prediction equation.

Table 2.2 Different types of packing with coefficients of friction factors

Packing	Type/size	Specific Area	Packing Density	C1	C2	C3	Reference
Structured packings							
Montz	B1 300	300	0.97	2	3	0.9	[27] , [28]
	B1 200	200	0.98	2	4	1.0	
	B1 100	100	0.99	3	7	1.0	
Gempack	2A	394	0.92	3	2.4	0.31	[24],[30]
	3A	262	0.93	3	2.3	0.28	[29]
Sulzer	Mellapak 250Y (plastic)	250	0.85	1	1	0.32	[33]
	Mellapak 250Y (metal)	250	0.96	5	3	0.45	[34]
	BX-packing	450	0.86	15	2	0.35	[34]
Dumped ceramic packings							
Raschig Rings	10	472	0.655	48	8	2.0	[31]
	10	327	0.657	10	8	1.8	
	15	314	0.676	48	10	2.3	
	15	264	0.698	48	8	2.0	
	30	137	0.775	48	8	2.0	
	35	126	0.773	48	8	2.15	
Pall Rings	25	192	0.742	10	3	1.2	[31]
	25	219	0.74	1	4	1.0	
	35	139	0.773	33	7	1.4	
	35	165	0.76	1	6	1.1	
Reflux Rings	50	120	0.78	75	15	1.6	[31]
Hiflow Rings	20	291	0.75	10	5	1.1	[26]
Berl Saddles	15	300	0.561	32	6	0.9	[35]
	35	133	0.75	33	14	1.0	
Intalox Saddles	20	300	0.672	30	6	1.4	[35]
	25	183	0.732	32	7	1.0	
	35	135	0.76	30	6	1.2	
Torus Saddles	25	255	0.73	19	1	0.85	
	50	120	0.75	10	8	0.75	
Dumped metal Packings: Raschig Rings	12	416	0.94	60	1	7.5	[31]

	15	317	0.924	40	1	6	
Pall Rings	25	215	0.94	0.05	1	3	[31]
	35	130	0.95	0.1	0.1	2.1	
Bialecki Rings	25	225	0.94	50	7	2.5	[29]
Nutter Rings	50	96.5	0.978	1	1	2.65	[29]
Cascade Mini Rings	25	230	0.96	-2	-2	2	[29]
Supersaddles	25	165	0.978	1	1.6	2.1	[29]
Dumped Plastic Packing's							
Pall Rings	90	71	0.95	-5	-4	2.3	[29]
NSW-Rings	25	180	0.927	1	1	1.35	[29]
Leva	1	190	0.92	1	1	2.0	[29]
	2	143	0.94	1	1	2.3	[29]

Ghosh et al., [35] in their study used 2 random namely 5/8 inch polypropylene flexi rings and Ceramic Berl saddles and 2 structured packing's of namely cross corrugated cellulose structured packing and PVC packing. Here they proposed the heat and mass transfer equation and they got the exponents of the equations from the experiments conducted on the given packing's. Here they also found that the flooding in Ceramic Berl saddles random packing occurs little early compared to structured packing at lower air flow rate due to less space for air flow. The heat transfer coefficient for the random packing was found always more compared to the structured packing.

Stichilmair et al. ,[29] has given the standard and different types of packing materials in their research article, that table given in article is reproduced here and contains the information about specific area, void fraction, friction factors and size and type of the packing material.

2.2.2 Effective surface Area for the Packing

Absorption phenomenon occurs at some spots on the packing materials. In real total area is not actually utilized for the absorption and some area is left out of effective absorption phenomenon making that area of no use for moisture removal. Viscosity , flow resistance, spraying of the solution, surface tension, flow rates pf fluids affect the effective surface area of the packing [30]. **Saeed et al.,** [30] in his simulation study used FLUENT model to predict the actual Effective surface area of the packing. In this paper he has proposed a relation for predicting the effective area. This relation is completely based on the model proposed by the Onda et al., [36] and Olujic et al., [27] which was given for random and Montz packing.

Onda et al.,[36] in their paper has given a relation for the effective packing area. They have considered the Counter-flow 2 phase Distillations Packed columns and their absorption and desorption; for the gas and liquid with packed bed columns. Onda et al., [36]in their paper has given this relation which is based on the experimental performance. This equation is a best line equation passing from the obtained data points. This equation given by the Onda et al., [36] is the most basic equation to obtain the actual area of the packing which takes part in absorption reaction.

$$a_{e,Onda} = a_p(1 - e^{-1.45\left(\frac{0.075}{\sigma}\right)^{0.75} Re_L^{0.1} Fr_L^{-0.05} We_L^{0.2}}$$

(2.1)

Rocha et al., [37] in their paper has used Flexipac-2 and Mellapak 250Y, BX packing proposed a relation for it. In his paper he did experimental investigation for the distillation column and for that they have proposed a general relation to get the value of the effective area for the packing and this relation is based on the geometric parameters of the packing. This relation can be used for the effective area prediction for the Metallic and ceramic Packing structures as paper the paper. Given expression has been tested for 0.02 bar to 4.14 bar.

$$a_e = a_t 1 - 1.203 \left(\frac{u_L^2}{Sg}\right)^{0.111}$$

(2.2)

S = side dimension of corrugation (m)

g =Acceleration due to Gravity

Here **Olujiae et al.,** [27] gave an expression involving an extra term which accounts for the unperforated packings with common size and pattern of holes such as used in Montz and Mellapak packing. Here they gave surface area void fraction as to be 10%. So in direct sense they reduced the total area by 10% of the installed area. This factor is related to the famous relation given by the Onda et al., [36] They have used the Delft Model for corrugated sheet structured packing for gas/ liquid phase. This equation has shown better accuracy than the its predecessor as per the author and shows less deviation than the actual.

$$a_e = (1 - \Omega)a_{e,Onda}$$

(2.3)

Ω = packing surface void fraction

$$a_{e,Onda} = a_p(1 - e^{-1.45\left(\frac{\sigma_c}{\sigma_L}\right)^{0.75} Re_L^{0.1} Fr_L^{-0.05} We_L^{0.2}})$$

(2.4)

$$R_{L,e} = \frac{\rho_L u_L}{\mu_L a_p} \tag{2.5}$$

$$W_{L,e} = \frac{\rho_L u_L^2}{\sigma_L a_p} \tag{2.6}$$

Saeed et al., [30]in their paper has proposed a relation for columns for Gemapak 2A packing. With the most basic relation given by the Onda et al. [36] and modified equation by Olujiae et al., [27] they proposed an improved version of this equation. They compared the output results with the data obtained from the Rocha et al., [37] Saeed et al., [30] validated the results of the of the model from the data obtained from the literature and found good agreement in the datasets.

$$n = \left(1 - \frac{a_p}{250}\right)\left(1 - \frac{a_{L,e}}{45}\right) + \ln\frac{a_{e,Onda}}{250} + (0.49 - \sqrt{\frac{0.101}{P}})(1.2 - \frac{a_{L,e}}{45}) \tag{2.7}$$

$$a_{L,e} = \cot(\frac{\cos(90-\beta)}{\sin(90-\beta)\cos\left(\cot\left(\frac{b}{2h}\right)\right)}) \tag{2.8}$$

β= angle of inclined corrugation to the horizontal

b= corrugation base dimension, m

h= corrugation crimp height, m

P= Pressure

2.3 Numerical Modeling

The basic heat exchange and mass transfer and its prediction is an important task. The temperature difference between the desiccant and air is the cause or potential for the heat transfer. The humidity exchange between the air and desiccant or to say the mass transfer is due to the difference between the vapor pressure of the desiccant and the air. Predication of the output data based on the input data is the main problem for any kind system and the same applies to the dehumidifier system. By knowing the properties of the given system which includes the geometric properties of the dehumidifier, air, desiccant allows us to predict the output parameters depending on input properties along with some boundary conditions.

In packed bed columns the prediction is based on the 3 basic models namely; finite difference method, NTU method, Simplified models. In the dehumidifiers process, some amount of heat is

given out. This heat is heat of dilution and the phase change heat. The heat of dilution is neglected while calculating the output parameters in all the dehumidifiers models. The reason for neglecting the dilution heat is that is its very small compared to the phase change model hence to reduce the complexity it is neglected[38].

Dehumidifiers can be classified into 2 types; adiabatic dehumidifiers and internally cooled dehumidifiers. Here in this study we are focused in the adiabatic dehumidifiers, as the setup exists and it's design is ready and easy [38]. In adiabatic dehumidifiers, the air and the desiccant come in direct contact and mix in a chamber. In spray chamber which was the center of the early research where the desiccant particles are broken down into small particles to increase the surface area of the liquid to increase the area of the heat and mas transfer. But sometimes the spray chambers may cause the problem of the fine particle carryover, and forms the mist and at some point cause the carryover problem hence the structured study was shifted to the different type of chambers famously known as the packed towers. These packed towers can provide the large surface area is compact can provide higher residence time and can lower the liquid pressure loss and carryover [38].

2.3.1 Finite Difference Method

In 1980 factor et al., [39] given a model to predict the performance of the dehumidifier. This model was proposed for the counter current flow arrangements of packed columns. This model was based on the theory of Adiabatic gas absorption given by Treybal in his famous book of 1969 [23].Only exception is that the resistance to the heat transfer in the liquid phase is negligible and neglected [26]. The assumption of this model are as follows:

- The flow of air and desiccant were assumed as the slug flow.
- The process happening in the dehumidifier was adiabatic
- The properties of the gas and liquid were assumed to be constant across the small differential element where the heat and mas transfer equations were solved.
- The specific area of heat and mass transfer area are equal and equal to the packing material specific area of the packing.
- Non-uniformity of the air was neglected.
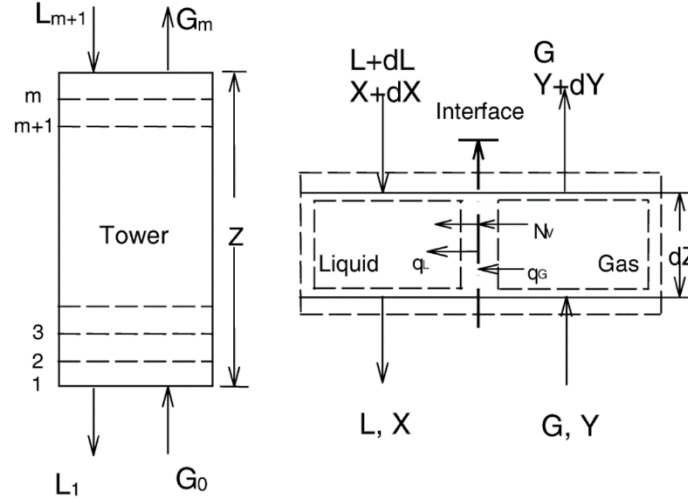
Figure 2.2 Packed Bed Dehumidifier Overview[26]

As shown in the schematic of the model the concentration gradient and temperature gradient exists only the z-direction. Only the water is transferred between the air and the desiccant. Here when we considered the LiCl solution one extra things need to be considered and it's that the solution has the high surface tension and hence the insufficient area is wetted and hence we need to consider this in the model while considering the insufficient wetting characteristics of the solution with the packing area. That equation is given by the Onda et al., [36] and that equation is further used for the calculation of the actual area.

$$a_w = a_{e,Onda} = a_t(1 - e^{-1.45\left(\frac{\sigma_c}{\sigma_L}\right)^{0.75} Re_L^{0.1} Fr_L^{-0.05} We_L^{0.2}})$$

(2.9)

$$R_{L,e} = \frac{\rho_L u_L}{\mu_L a_p}$$ (2.10)

$$W_{L,e} = \frac{\rho_L u_L^2}{\sigma_L a_p}$$ (2.11)

$$Fr_L = \frac{a_p u_L^2}{g}$$ (2.12)

The above equation takes into account the liquid surface tension and surface energy of packing materials [26].The K type mass transfer coefficient are given as follows;

$$K_L = 0.0051 \left(\frac{\mu_L g}{\rho_L}\right)^{0.3333} \left(\frac{L}{a_w \mu_L}\right)^{0.6667} \left(\frac{\rho_L D_L}{\mu_L}\right)^{-0.05} \left(a_t D_p\right)^{0.4}$$ (2.13)

$$K_G = 5.23 \left(\frac{a_t D_G}{RT_a}\right) \left(\frac{G}{a_t \mu_G}\right)^{0.7} \left(\frac{\mu_G}{\rho_G D_G}\right)^{0.3333} \left(a_t D_p\right)^{-2} \tag{2.14}$$

Then the equations for the humidity change as per the Goswami paper [41] are;

$$\frac{dY}{dZ} = -\frac{M_W F_G a_W}{G} \ln \frac{1-Y_i}{1-Y} \tag{2.15}$$

$$\ln \frac{1-Y_i}{1-Y} = \ln \frac{1-\left(\frac{P_S}{P_t}\right)}{1-\left(\frac{P_a}{P_t}\right)} \tag{2.16}$$

Where the interfacial gas phase concentration can be calculated by the following equation:

$$Y_i = 1 - (1-Y)\left(\frac{x}{x_i}\right)^{\frac{F_L}{F_G}} \tag{2.17}$$

The K type of mass transfer equations can be transformed into the F- type mass transfer coefficients and that can be done by the following equation:

$$F_L = K_L x_{SM} \frac{\rho_L}{M_L} \tag{2.18}$$

Interfacial concentration can be considered equal to 1 for very dilute solutions. For lithium chloride the logarithmic mean desiccant mole fraction difference amongst the bulk liquid, interface values can be calculated from the following equation:

$$x_{SM} = \frac{x - x_i}{\ln \frac{x}{x_i}} \tag{2.19}$$

The gas phase the K type mass transfer coefficient can be converted to the F-type mass transfer coefficient as follows:

$$F_G = K_G P \tag{2.20}$$

From above equations we can calculate the change in the air temperature across the taken differential element and that can be given by the following equation [42]:

$$\frac{dT_a}{dz} = \frac{h_G' a_t (T_L - T_L)}{G(c_{p,a} + Y c_{p,v})} \tag{2.21}$$

Where the heat transfer term is corrected for the simultaneous heat and mass transfer and it's given by:

$$h'_G a_t = \frac{-G c_{p,v} \frac{dY}{dz}}{1 - exp\left(\frac{G c_{p,v} \frac{dY}{dz}}{a_t \, h_G}\right)}$$

(2.22)

The heat transfer coefficient in the above equation can be found by the following equation:

$$h_G = F_G M_a (c_{p,a} + Y c_{p,v}) \frac{Sc^{0.667}}{Pr^{0.667}}$$ (2.23)

Where $Sc = \frac{\mu_G}{\rho_G D_G}$ (2.24)

From this above equation we can get the change in the desiccant flow rate and the concentration change and temperature change across the finite element. The equations for the change of parameters are as follows:

$$\frac{dL}{dz} = G \frac{dY}{dz}$$ (2.25)

$$\frac{dx}{dz} = -\frac{G}{L} x \frac{dY}{dz}$$ (2.26)

$$\frac{dT_L}{dz} = \frac{G}{c_{p,L}L}\left\{(c_{p,a} + Y c_{p,v}) \frac{dT_a}{dz} + \left[c_{p,v}(T_a - T_0) - c_{p,L}(T_L - T_0)\frac{dY}{dz}\right]\right\}$$

(2.27)

In the whole of the all equations are governed by the vapor pressure difference and it's the most important characteristics of the system. Above all the equations are governed by the humidity differential element segment slope and that equation is governed by the equilibrium humidity ratio at desiccant surface.

2.3.2 Number of Transfer Units Method

An effective model which was developed for the liquid desiccant heat and mass transfer. This model was modified from the simple effectiveness model for the cooling towers[38][43]. This model was based on the same assumptions with 2 more extra additives ones and those are:

- Linear variation of the saturation enthalpy and temperature
- To neglect the water loss energy in energy balance
- Effective heat and mass transfer was assumed

The following steps are followed for the NTU Model;

To calculate the NTU:

$$NTU = \frac{F_G a_t V M_a}{G} \tag{2.28}$$

From above definition we can calculate the effectiveness of the dehumidifier which is analogous to the counter-current flow Heat Exchanger and hence we can put forward below formula:

$$\varepsilon = \frac{1 - \exp(-NTU(1 - m^*))}{1 - m^* \exp(-NTU(1 - m^*))} \tag{2.29}$$

$$m^* = \frac{G c_{p,a,sat}}{L c_{p,v}} \tag{2.30}$$

With above equations we can calculate the air outlet enthalpy as follows:

$$h_{a,o} = h_{a,i} + \varepsilon(h_e - h_{a,i}) \tag{2.31}$$

From above equation knowing the inlet and outlet enthalpy will give us the total enthalpy change and from that we can calculate the outlet solution enthalpy by the energy balance. From here we can get the effective saturation enthalpy and that can be found as:

$$h_{e,eff} = h_{a,i} + \frac{(h_{a,o} - h_{a,i})}{1 - \exp(-NTU)} \tag{2.32}$$

From above parameters we can get the outlet humidity:

$$Y_o = Y_{e,eff} + (Y_e - Y_{e,eff}) \tag{2.33}$$

With the mass balance we can found out the other remaining parameters of the solution and air.

2.3.3 Simplified Models

Finite difference and NTU model require some amount of computation; both are iterative method. Thus takes lot of time and resources and not suitable for the hourly performance evaluation. Simplified models are the equations developed over an extensive dataset which are related to the input datasets for output data; But these data sets are developed with FDM datasets and hence they are suitable only for some range of the input values.

2.3.4 Difference Between the Different Numerical Models

Table 2.3 Comparison of different types of the Numerical Modeling methods

Model	Assumptions	Iteration	Accuracy
FDM Model	Least	Most	Best
NTU Model	More	Lesser	Better
Simplified Model	Most	No	Depends on datasets

2.4 Pressure Drop Prediction

In dehumidifier the packing material create obstruction for the flow of the air and hence we need to see how much amount of energy is lost in making the circulation of the air in dehumidifier. When the packing is dry and when the desiccant is flowing both has different pressure drops. The pressure drop is increased when the liquid flows through that packing. This increase of the pressure drop when the packing is irrigated due to the fact that liquid is being held up in the packing this changes the effective structure of the bed; as porosity is decreased [29].This leads to increase in the friction between fluid flow and increase in the fluid particle. Packing pressure drop is function of packing type, height, diameter of the packed bed also depends on the desiccant and air mass flow rates [24].Structured packing results in lesser pressure drop compared to the random packing as per the Gandhidasan study.

There are three flow operating characteristics that we need to consider while studying this pressure model. When the flow rate of air is varied while keeping the desiccant flow rate constant shows that the pressure drop increases rapidly as if the packing was not made wet. That shows the desiccant flow rate has not that much effect when compared to the air flow rate on pressure drop. When the liquid flows through the packing materials the flow characteristics make the liquid to stay in the voids this liquid is held inside the cavity and hence known as the dynamic holdup or operating holdup. When the air flow rate is significantly increased such that significant amount of liquid is held inside the packing we call that point as the loading point of the packing. This loading occurs as the packing's area decreases with increasing loading and void space becomes smaller. The point when the desiccant remains accumulated above the top side of packing we say that the packing is flooded. In this region the pressure drop increases rapidly. The value of air flow rate at which this condition occurs we call that point as the flooding point [24]. Stichilmair et al., [29] in their paper has used particle model for knowing the expected pressure drop in the packing. They used this model with structured and random packing. This model first predicts the dry pressure

drop and adds an extra arrangement for the pressure drop due to the liquid holdup. Castillo et al., [32] has used the model provided by the Stichilmair et al., [29] and did some modifications for liquid holdup, irrigated and flooding pressure drop predication [32].

The model requires the equivalent diameter or which is also knows as the equivalent characteristics dimensions of the packing and that packing is related with the void fraction and the specific surface area which are most of the time is provided by the manufacturer. From Treybal [23] we can get the equation for the equivalent diameter and it's given as:

$$D_P = \frac{6(1-\epsilon)}{a_t} \qquad (2.34)$$

Above equation can be replaced by the more basic equation which involves the using actual dimensions of the packing includes crimp height, channel base ,channel side which was given by the Bravo et al.,[37].

$$D_P = \frac{Bh}{S} \qquad (2.35)$$

The dry be pressure drop based on the analogy considering the fluidized bed and it's given by:

$$\Delta P_d = 0.125 f_0 \frac{\rho_G u_G^2 a_t}{\epsilon^{4.65}} \qquad (2.36)$$

Where the friction factor depends on the type of the packing. This data for calculating the friction factor is given by the Stichilmair et al., [29] in his paper.

$$f_0 = \frac{C_1}{Re_G} + \frac{C_2}{Re_G^{0.5}} + C_3 \qquad (2.37)$$

$$Re_G = \frac{\rho_G D_P u_G}{\mu_G}$$

The Constant of C_1, C_2, C_3 vary with the type of the packing. Liquid holdup is the important parameter that related the pressure drop and mass transfer efficiency and capacity of the system. Liquid holdup depends on the shape and nature of the packing, flow rates and some liquid physical properties. This liquid holdup has two components namely static and dynamic holdup. Holdup can be simple defines as the volume of liquid in the packing per unit volume of packing. As the flow rate in increases it increases the dynamic holdup and the static holdup remains constant and a point is reached when the static holdup become of less significance compared to the operating holdup.

Static holdup is responsible for the mass transfer process in the dehumidification process and is constantly replaced to maintain the equilibrium in the process. Below the loading point the operating holdup depends on the superficial velocity of the desiccant. The static holdup is given by the following formula:

$$h_b = 3.6 \left(\frac{u_L a_t^{0.5}}{g^{0.5}}\right)^{0.66} \left(\frac{\mu_L a_t^{1.5}}{\rho_L g^{0.5}}\right)^{0.25} \left(\frac{\sigma_L a_t^{2.0}}{\rho_L g}\right)^{0.1} \qquad (2.38)$$

When we cross the loading point then the operating liquid holdup is the function of the irrigated or total pressure drop and which can be given by the following equation:

$$h_a = h_b \left[1 + \left(\frac{6\Delta P_{irri}}{\rho_L g}\right)^2\right] \qquad (2.39)$$

In order to find the irrigated pressure, drop it is necessary to find the diameter of the falling liquid particles and that can be calculated by the equating the surface tension force to the inertia force and it is given by the following equation:

$$d_L = C\sqrt{\frac{6\sigma_1}{(\rho_L - \rho_g)g}} \qquad (2.40)$$

Where the C=0.8 for the structured pickings and C =0.4 for the random packing

The effective surface area offered by the liquid particles is given by the following equations:

$$a_L = 6\frac{h_a}{d_L} \qquad (2.41)$$

The irrigated or the total pressure drop can be calculated by the following equation:

$$\frac{\Delta P_{irri}}{\Delta P_{dry}} = \left(\frac{a_L + a_t}{a_t}\right)\left(\frac{\epsilon}{\epsilon - h_a}\right)^{4.65} \qquad (2.42)$$

Above equation involves 2 unknowns and hence iterative procedure needs to adopted and to get the dynamic holdup and total pressure drop. At starting point, the total pressure can be assumed to be equal to the dry pressure drop and hence total pressure can be found in response. The above equation is fully applicable to the types of the pickings namely random and structured pickings.

The dehumidifier column and its dimensioning involve the flooding point and that can be calculated with applying following equation. The equation is derived by taking derivative where

26

the total pressure drop tends to infinity at the flooding point and hence can be solved for the flooding pressure drop.

$$\Delta P_f = \frac{\rho_L g}{2988 h_b} \sqrt{249 h_b \left(\sqrt{X} - 60\epsilon - 558 h_b - 103 d_L D_P\right)} \tag{2.43}$$

Where flooding coefficient in the above equation can be calculated as follows;

$$X = 3600\,\epsilon^2 + 186500\,\epsilon h_b + 32300 d_L a_t \epsilon + 191800 h_b{}^2 + 95030 d_L a_t h_b + 10610 d_L{}^2 a_t{}^2 \tag{2.44}$$

2.5 Liquid desiccant as a heat transfer Fluid

2.5.1 Lithium chloride LiCl

In 1992 **Anderson et al.** , [44] in his paper has explained the properties of the lithium chloride as a liquid desiccant for dehumidification. LiCl is the most stable desiccant and it has been observed that it has high dehydration concentration of around 30%-45%. In his paper he claimed that the dehumidification capacity of the solution is high as 15%. Apart from its good performance characteristics, the cost at that time was high, around 9-13 $ USD/kg(25000 $USD/ton) which was quite high and hence he proposed a mixture of calcium chloride such that the balance between the cost and performance can be achieved .

Bouznanda et al. , [45] in their experimental work has shown that the performance of the LiCl is better when it is used in dehumidification process and $CaCl_2$ has better characteristics when operated for regeneration process. Lithium chlorides solution need to have high partial pressure of water just above the solution as when air which has lower vapor pressure comes in contact creates a potential difference in the partial vapor pressure for the required dehumidification; this partial vapor pressure difference is the driving force for the dehumidification. Hence the performance of the desiccant system depends on the desiccants vapor pressure. The vapor pressure of the 100% $LiCl_2$ solution and its vapor pressure variation with temperature is shown below.
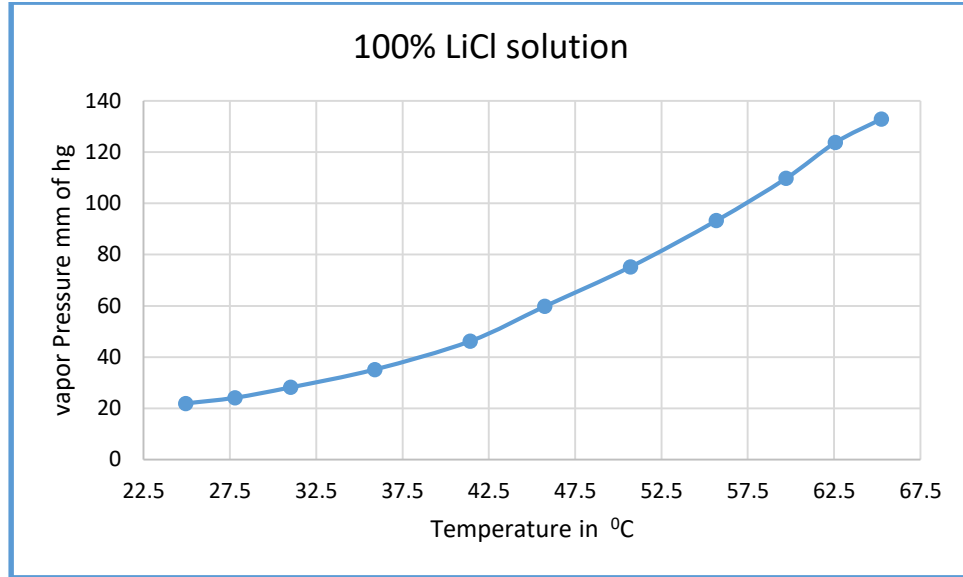
Figure 2.3 Variation of Vapor pressure of LiCl solution with temperature [32]

Nelson et al. , [26] in 2002 carried out an experiment and compared the data with finite difference model, in which he clearly showed how dehumidification with LiCl solution is a strong function of desiccant concentration, temperature, air flow rate, air humidity ratio. In this study he also mentioned that desiccant temperature , concentration, airflow rate has the greatest impact on the design of regenerator.

The overall heat transfer in the system occurs at the constant pressure so the addition of the other enhancers may increase or decreases the thermo-physical properties of the solution as explained by the **Yijan et al.**, [47] in his observation done on the scanning calorimeter with different solutions.

Sabek et al., [48] in his performance investigation has been done on the properties of air and lithium chloride solution which are separated by the porous membrane. In this study he found out that the optimal velocity of inlet air and desiccant liquid has significant impact on heat and mass transfer rates as well on the latent, sensible heats and heat transfer effectiveness. Humidity of inlet air also has a great impact on the mass and heat transfer rates in the desiccant liquid air membrane energy exchanger [48] [49]. The variation of the isobaric specific heat of base LiCl solution is as follows,
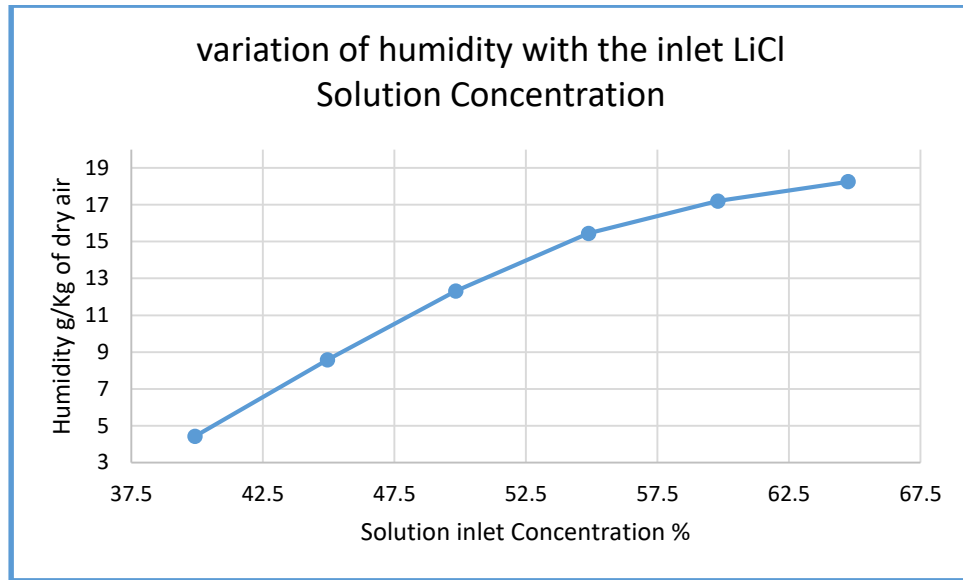
Figure 2.4 Variation of humidity with the inlet LiCl [34]

Table 2.4 Isobaric Heat capacity of LiCl Solution with different mixtures

Sr. No.	Desiccant solution	Isobaric Specific heat(kJ/kg.K)	Temperature (K)
1	(15% to 45%) LiCl + H2O	2.649-2.729	308.15-343.15
2	Lithium chloride(10%-23.3%) + tri-ethylene glycol (TEG) 20%-46.7%) + water	2.640-2.752	308.15-343.15
3	Lithium chloride(10%-23.3%) + propylene glycol (PG)(20%-46.7%) + water	2.663-2.775	308.15-343.15

Guo et al., [50] carried out experiments on the aqueous lithium chloride (LiCl) solution, using electro-dialysis for regeneration and he found that with increase in the flow rate the regeneration capability decreases and concentration difference has great effect on the system performance.

Wen et al. , [51] studied and compared the LiCl with KCOOH and found that LiCl performs much better when compared to the KCOOH, as the performance given by the 70.3% KCOOH is same as that of 35% LiCl solution when compared the vapor pressure.

2.5.2 Calcium Chloride CaCl₂

Anderson et al. , [44] in his comparative study has shown that the $CaCl_2$ can be an option for dehumidification as it has lower cost compared to the LiCl but has a lower performance characteristic which can be seen from the below mentioned graph and hence $CaCl_2$ need to be use along with the LiCl solution. While comparing the solutions he found that LiCl solely can't be compared on the basis of the vapor pressure characteristics we need to compare on the basis of the concentrations as well [45].
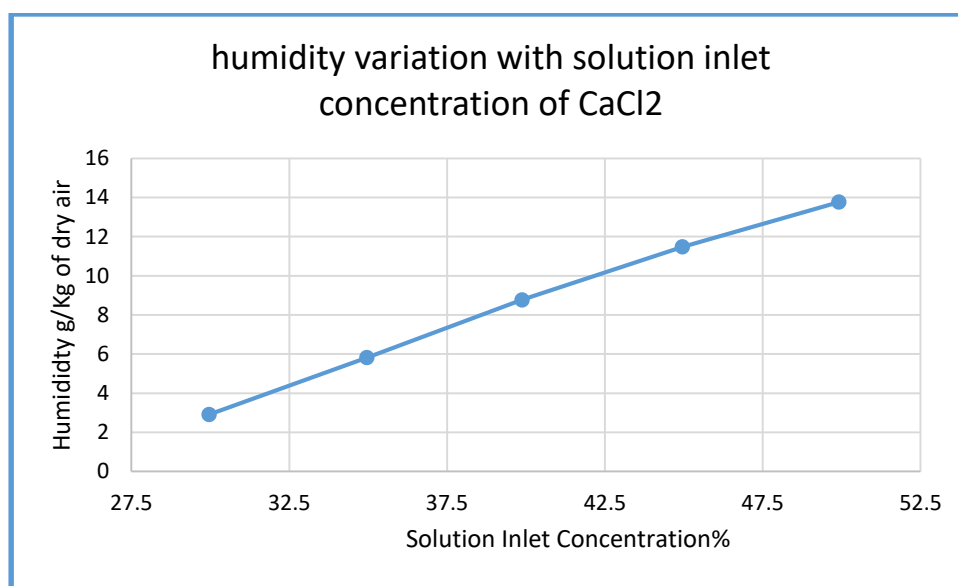
Figure 2.5 Humidity variation with solution inlet concentration of CaCl₂ [34]

In his CELD (Cost-Effective Liquid Desiccant) solution he has observed that 26.8 wt% mixture has the same vapor pressure as of a 20 wt% concentration LiCl solution which corresponds to the 30% reduction in the cost, the further reduction in cost up to 50% is possible by employing the CELD solution instead of LiCl solution while operating at higher flow rates [44]. LiBr is also a good desiccant solution but it has problem of uneven performance profile and it can be reduced by using the $CaCl_2$ as a constitute of mixture [52].

Bhowmik et al. , [53] in their numerical study has shown that using $CaCl_2$ as a constitute has shown a good trade of between the cost and performance 5% $CaCl_2$ and 35% LiCl has shown the comparable performance with pure LiCl.
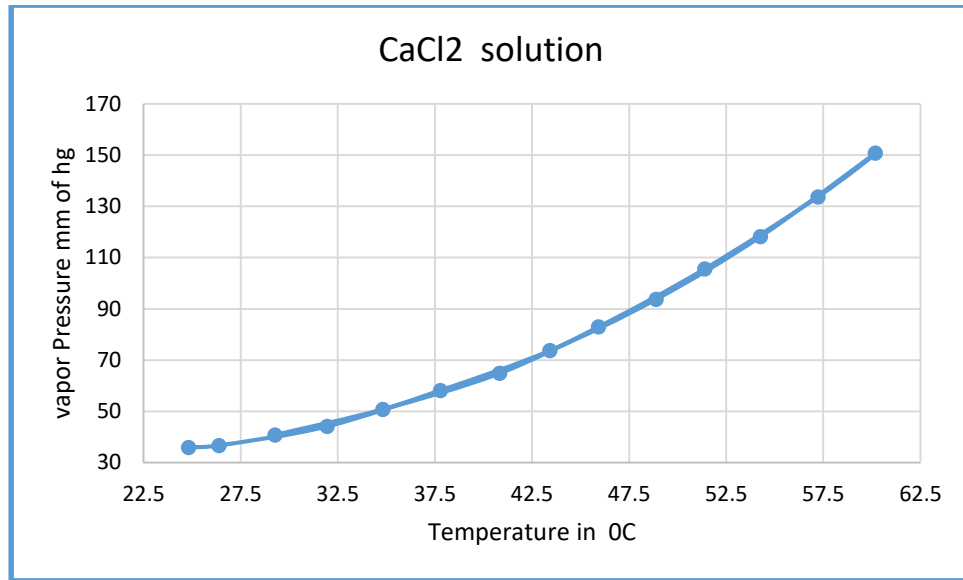
Figure 2.6 Variation of Vapor pressure of 100% CaCl2 solution with temperature [34]

2.5.3 Lithium Bromide LiBr

LiBr possess low water vapor pressure due to which it is being used for the desiccant solutions but have the drawback of corrosion. The problem of corrosion can be solved by adding the formate salts into the solution of the LiBr/LiCl [53][54].

Xu et al., [55] in their analysis used the LiBr for absorption refrigeration system and LiCl for dehumidification process and they found the good effect of this cascade system and their systems maximum COP was around 0.6029 and moisture removal rate was around 20.20g/kg and 0.9385 humidity efficiency. It has been observed that increasing the concentration of the LiBr from 15wt% to 60wt% in solution at temperature lesser that 373K, enhances the rate of absorption while decreasing the LiBr+H2O liquid-vapor interfacial layer thickness.

2.5.4 Formates

Mostly two formates are being utilized for the dehumidification and they are the Potassium and sodium format KCOOH, NaCOOH. Formates are low cost organic materials which can be used to improve the performance of the solution mixture[56].The halide solutions have a problem and that is the problem of corrosion and crystallization at high concentrations and requirement of high energy for regeneration and this can be reduced by using the formates in the solution.

The optimum amount of formates is really important as the absorption rate depend upon the optimum quantity of the CH2ONa in the LiBr solution as stated by the **Lidong et al.** , [54] in their numerical model. This enhanced absorption characteristic is due to the molecular clustering to be more specific due to the Li+ and COOH- ions tend to form the clusters which create the cavity structure which holds the water molecule inside that cluster. It has been observed that the mixtures such as the LiBr+CH$_2$ONa at 45% by mass with some added constituents such as n-Octanol has shown improved results when compared with LiBr solution[52][56].

2.5.5 Tri Ethylene Glycol (TEG)

TEG has been used by the **Fakharnezhad et al.,** [57] in their experiment and found that it has been effective in their design for moisture removal from the gas, here they have used the polyvinylidene fluoride and polypropylene hollow fiber membrane contactors with TEG as the absorbent material and have shown effective dehumidification characteristics.

Table 2.5 Different Liquid desiccant and their price in $ USD per ton [58]

Sr. No.	Liquid Desiccant	Salt form	Price per metric Ton ($ USD)
1	Lithium chloride (LiCl)	Anhydrous	7400
2	Calcium Chloride (CaCl2	Di-hydrate	284
3	Lithium bromide (LiBr)	Anhydrous	3660
4	Magnesium chloride (MgCl2)	Hexa-Hydrous	155
5	Tri-ethylene glycol (TEG)	-	Cheaper than aqueous salt 1625
6	Calcium chloride-Lithium chloride mixture (CaCl2-LiCl)[CELD]	Aqueous Solution	30% lower than LiCl
7	Propylene Glycol (PG)	-	Costlier than halide salts, 1812
8	Formates		2200

Table 2.6 Different Desiccants and their Comparison

Parameters	Vapor pressure	Absorption Water Capacities (Relative)	Viscosity	Relative Cost and stability	Dehumidification Performance	Regeneration Temperature	Corrosiveness	Crystallization	Optimum operating concentration levels	Technology
CaCl2	Compare to LiCl & LiBr its higher	Lowest	Low	Cheaper & available but unstable	Lower than LiCl	Below 80 °C	Corrosive	Crystallized	35-45%	
LiCl	Lowest in all halide salts	11% Higher than CaCl2	low	Very expensive, most stable	Better than CaCl2 and LiBr	Below 85 °C	less Corrosive	Crystallized	30-45%	
LiBr	Higher	6% Lesser than LiCl	low	Cheaper than LiCl	Lower than LiCl	Below 80 °C	Corrosive	Crystallized	45-60%	
LiCl & CaCl2(CELD)	Lower than the CaCl2		low	Saving about 30%					95-97%	
MgCl2		Weaker		Low cost, easily availability, lesser toxic				More Crystallized		
TEG	surface vapor pressure is Very low	volatile	high	Unstable, more Cost		Below 80 °C	Not corrosive and Material		90-98	Earliest used
HCOOK				Cheaper than aqueous salt	Effective above Moisture content	Vary according to flow rates; from 45°C-	Less corrosive and Environmen		65-70%.	New liquid desiccant
Glycol-Water Solution (MEG,	Low	volatile	high	Expensive	Higher dehumidification	Low regeneration than saline solution	Lower corrosive			New organic compounds
References	[59]	[60]	[61]	[60]	[60]	[62]	[60][62][63][64]	[60][62][63][64]	[62]	[65]

2.6 Summary of the literature survey

- Structured packing materials has better heat and mass transfer characteristics compared to the random packing materials.

- Friction factor in dry pressure drop varies with the packing material type. Therefore, it is necessary to choose right packing material according to the need.

- The actual area for the effective absorption is different. It is necessary to choose proper effective area calculating equation for the packing. Here we have chosen Onda et al., [36] famous equation for calculating the effective area of the packing material.

- The FDM model is gives better performance compared to other models for dehumidifier performance prediction.

- Pressure drop depends on the packing type and its geometry and hence need to be chosen with proper care. Pressure drop depends on the liquid holdup. This liquid holdup also gives the direction for the proper design of the system based on the flooding property.

- LiCl shows best results for the dehumidification but it is costly. The mixtures of the desiccant may give better performance characteristics.

Chapter-3

NUMERICAL STUDY

Predicting the performance of the dehumidifier based on the input has been an important step in reducing the real-time based cost. Experiments can be costly and hence it's really important to tests the given conditions with some models which will simulate the problem statement with some assumptions and approximations to the actual conditions. This study helps in reducing the time and allows to allocate the resources in right amount. Here we have tried to make a model for prediction of the dehumidifier performance with specific humidity model with finite difference method. Here we have also tried to make a model which will predict the pressure loss in the packing and hence will allow us to say and choose best packing's for lesser pressure losses. Here we have tried to use and verify the work of the Al-Farayadhi et al.,[25] in which they have given the relation for the mass transfer coefficients for both phases and along with the heat transfer coefficients.

3.1 FDM Model for Predicting the Dehumidifier Performance

Finite difference model is the most accurate model as per the literature. It divides the region in the many segments and studies the variation of the properties in that element which are utilized in the next subsequent element for the output properties. This allows to change the properties and dynamic transfer is considered which allows to change the driving potentials which drives the heat and mass transfer.

3.1.1 Problem Statement

For the consideration of the problem the work of the **Goswami et al.,** [26] is considered. The dehumidifier with the 0.254m diameter and 0.60 m height cylindrical column was considered. The packing materials was Polypropylene Rauschert Hiflow Rings with surface area of 210 m2/m3 was considered. The desiccant solution considered was of LiCl. The model considerations include the adiabatic chamber. The inlet properties were known and the outlet properties based on the inlet properties were calculated. Below shown schematics shows the dehumidifier finite elements considerations and how the heat and mass transfer is considered.
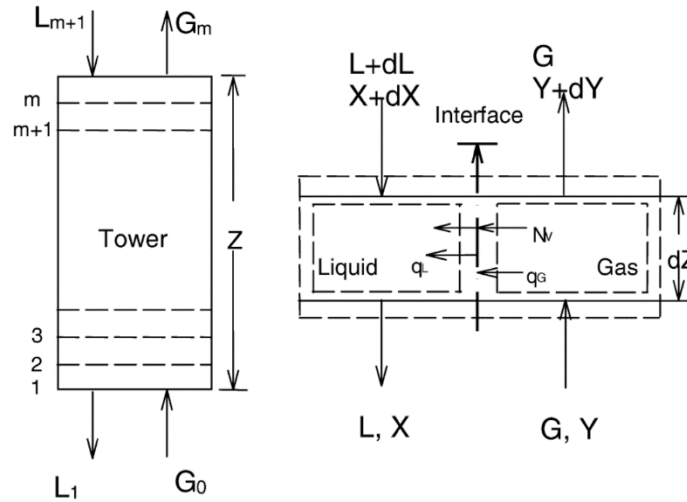
Figure 3.2 Packed Bed Dehumidifier Overview [26]

3.1.2 Assumptions

- The flow of air and desiccant were assumed as the slug flow.
- The processes are adiabatic.

- The properties of the gas and liquid were assumed to be constant across the small differential element where the heat and mas transfer equations are solved.
- The specific area of heat and mass transfer area are equal and equal to the packing material specific area.
- Non-uniformity of the air was neglected.

3.1.3 Governing Equations

To calculate the actual wet area following equation is used in the model:

$$a_w = a_{e,Onda} = a_t(1 - e^{-1.45\left(\frac{\sigma_c}{\sigma_L}\right)^{0.75}Re_L^{0.1}Fr_L^{-0.05}We_L^{0.2}})$$

$$R_{L,e} = \frac{\rho_L u_L}{\mu_L a_p}$$

$$W_{L,e} = \frac{\rho_L u_L^2}{\sigma_L a_p}$$

$$Fr_L = \frac{a_p u_L^2}{g}$$

The K type mass transfer coefficient are given as follows;

$$K_L = 0.0051 \left(\frac{\mu_L g}{\rho_L}\right)^{0.3333} \left(\frac{L}{a_w \mu_L}\right)^{0.6667} \left(\frac{\rho_L D_L}{\mu_L}\right)^{-0.05} \left(a_t D_p\right)^{0.4}$$

$$K_G = 5.23 \left(\frac{a_t D_G}{RT_a}\right) \left(\frac{G}{a_t \mu_G}\right)^{0.7} \left(\frac{\mu_G}{\rho_G D_G}\right)^{0.3333} \left(a_t D_p\right)^{-2}$$

Then the equations for the humidity change is:

$$\frac{dY}{dZ} = -\frac{M_W F_G a_W}{G} \ln\frac{1-Y_i}{1-Y}$$

$$\ln\frac{1-Y_i}{1-Y} = \ln\frac{1-\left(\frac{P_S}{P_t}\right)}{1-\left(\frac{P_a}{P_t}\right)}$$

The K type of mass transfer equations can be transformed into the F- type mass transfer coefficients as follows:

$$F_G = K_G P$$

$$F_L = K_L x_{SM} \frac{\rho_L}{M_L}$$

$$\frac{dT_a}{dz} = \frac{h_G' a_t (T_L - T_L)}{G(c_{p,a} + Y c_{p,v})}$$

$$h_G' a_t = \frac{-G c_{p,v} \frac{dY}{dz}}{1 - exp\left(\frac{G c_{p,v} \frac{dY}{dz}}{a_t h_G}\right)}$$

The heat transfer coefficient in the above equation can be found by the following equation:

$$h_G = F_G M_a (c_{p,a} + Y c_{p,v}) \frac{Sc^{0.667}}{Pr^{0.667}}$$

Then the variation of the mass, concentration, Temperature of desiccant and can be found from the following equations:

$$\frac{dL}{dz} = G \frac{dY}{dz}$$

$$\frac{dx}{dz} = -\frac{G}{L} x \frac{dY}{dz}$$

$$\frac{dT_L}{dz} = \frac{G}{c_{p,L} L} \left\{ \left(c_{p,a} + Y c_{p,v} \right) \frac{dT_a}{dz} + \left[c_{p,v} (T_a - T_0) - c_{p,L} (T_L - T_0) \frac{dY}{dz} \right] \right\}$$

The above equations and the properties of the liquid desiccant can be found from the Conde et al., [36] paper and has been used here.

3.1.4 Properties of the LiCl desiccant Solution

3.1.4.1 Surface tension of the LiCl solution

Surface tension is the force acting on the surface of a liquid. When the area of contact in liquid phase made to reduce it, the force which tries to reduces this area is called the surface tension. The LiCl solution has more surface tension that water. This extra account for the LiCl adds to enhance the equation for the surface tension of the solution. Surface tension of the water is calculated with the IAPWS equations. This surface tension of water is then modified for the account of the concentration of LiCl solution. Conde et al., [36] has done experimental extensive research on the LiCl solution has given the following formula:

$$\sigma_{H2O}(\theta) = \sigma_0 (1 + b(1 - \theta))(1 - \theta)^\mu) \tag{3.1}$$

$$\sigma_{sol}(\theta, x) = \sigma_{H2O}(1 + \sigma_1 x + \sigma_1 x\theta + \sigma_2 x\theta + \sigma_3 x\sigma_2\theta^2 + \sigma_4 x^2 + \sigma_5 x^3) \tag{3.2}$$

$$\theta = \frac{T_L(°C) + 273.15}{T_C(°C) + 273.15} \tag{3.3}$$

$$T_c°C + 273.15 = 647.6K$$

T_c = critical Temperature of the water = 647.3K

Table 3.1 The coefficient of the formula of the surface tension of LiCl solution

σ_1	σ_2	σ_3	σ_4	σ_5	σ_0(mN/m)	μ	b
2.757115	-12.0113	14.75182	2.443204	-3.14774	235.8	1.256	0.625

3.1.4.2 Density of LiCl Solution

The density of the solution increases with the increase in the solution concentration. It is related with the solution temperature and the solution concentration. The more the concentration the more the salt concentration and hence increase the density of the solution. The formula to calculate the density of the solution is as follows;

$$\rho_{sol}(x, T_L) = \rho_{H2O}(T) \sum_{i=0}^{i=3} \rho_i \left(\frac{x}{1-x}\right)^i \tag{3.4}$$

$$\rho_{H2O}(T) = \rho_{0,H2O}\left(1 + B_0\tau^{\frac{1}{3}} + B_1\tau^{\frac{2}{3}} + B_2\tau^{\frac{5}{3}} + B_3\tau^{\frac{16}{3}} + B_4\tau^{\frac{43}{3}} + B_5\tau^{\frac{110}{3}}\right) \tag{3.5}$$

$$\tau = 1 - \frac{T_L(°C) + 273.15}{T_C(°C) + 273.15}$$

Table 3.2 The coefficient of the LiCl solution density formula

B_0	B_1	B_2	B_3	B_4	B_5
1.993772	1.098521	-0.50945	-1.76191	-45.9005	-723692
ρ_0	ρ_1	ρ_2	ρ_3		
1	0.540966	-0.303792	0.100791		

3.1.4.3 Thermal Conductivity of LiCl Solution

The data provided by the Uemura is related with the concentration and the temperature of the solution. It is studied that this data is not that much accurate and can be modified for better accuracy. Here the thermal conductivity of the water is related to the thermal conductivity of the solution.

$$\propto_r = \frac{\lambda_{H2O}(T_L) - \lambda_{sol}(T_L, x)}{\zeta_{eq}}$$

(3.6)

$$\zeta_{eq} = \frac{x \rho_{sol}(x, T_L)}{M}$$
(3.7)

$x = mass\ fraction\ of\ the\ solution$

$\lambda_{H2O}(T_L) = thermal\ conductivity\ of\ the\ pure\ water$

$\propto_r = \propto_0 + \propto_1 x$

$\propto_0 = 0.010896$

$\propto_1 = -0.01179$

$\nabla_{H2O}(\theta) = \nabla_0(\tau)\nabla_L(\delta, \tau)$

$\nabla_0(\tau) = 1/[\tau^{0.5} \sum_{i=0}^{i=3} n_i^0 \tau^i]$

$\nabla_L(\delta, \tau) = exp[\delta \sum_{i=0}^{4} \sum_{j=0}^{5} n_{ij}(t-1)^i(\delta-1)^j]$
(3.8)

$\nabla = \frac{\lambda}{\lambda^*}$

$\lambda^* = $ Critical thermal conductivity of water in W/mK

$\delta = \frac{\rho}{\rho^*}$

$\rho^* = $ Critical density of the Water in $Kg.\,m^{-3}$

$\tau = \frac{T}{T^*}$

Table 3.3 Coefficient of thermal conductivity of LiCl solution

n_0^0	n_1^0	n_2^0	n_3^0
1	6.978267	2.599096	-0.99825

Table 3.4 Coefficient of thermal conductivity of LiCl solution

j	$n_{0,j}$	$n_{1,j}$	$n_{2,j}$	$n_{3,j}$	$n_{4,j}$
0	1.329305	1.701836	5.224616	8.712768	-1.8526
1	-0.40452	-2.21568	-10.1241	-9.50006	0.934047
2	0.244095	1.651106	4.987469	4.378661	0
3	0.018661	-0.76736	-0.27298	-0.91784	0
4	-0.12961	0.372833	-0.43083	0	0
5	0.04481	-0.11203	0.133385	0	0

3.1.4.4 Specific heat of the LiCl Solution

The specific heat of the LiCl solution is calculated based on the specific heat of the water solution. This specific heat is the function of the concentration and temperature of the desiccant solution. The formula to calculate the specific heat of the solution is given as follows:

$$C_{p,sol}(T,x) = C_{p,H2O}(1 - F(x)G(T)) \tag{3.9}$$

$$C_{p,H2O} = A + B\theta^{0.02} + C\theta^{0.04} + D\theta^{0.06} + E\theta^{1.8} + F\theta^8 \tag{3.10}$$

$$F(x) = Ax + Bx^2 + Cx^3$$

$$G(T) = F\theta^{0.02} + G\theta^{0.04} + H\theta^{0.06}$$

$$\theta = \frac{T(°C)}{228} - 1 \tag{3.11}$$

Table 3.5 Coefficient of specific heat formula for LiCl solution

A	B	C	D	E	F	G	H
1.4398	-1.24317	-0.1207	0.12825	0.62934	58.5225	-105.634	47.7948

3.1.4.5 Saturated Vapor Pressure of the LiCl Solution

The most important parameter which determines the pattern of humidity changes in the dehumidifier. Humidity slope which has the term of saturated pressure and that slope defines and drives all the dehumidifier equations. To determine the saturated pressure at the solution concentration and temperature a formula was put forth and its given below[66];

$$\pi = \frac{P_{sol}(x,T)}{P_{H2O}} = \pi_{25}f(x,\theta) \tag{3.12}$$

$$f(x,\theta) = A + B\theta$$

$$A = 2 - \left[1 + \left(\frac{x}{\pi_0}\right)^{\pi_1}\right]^{\pi_2}$$

$$B = \left[1 + \left(\frac{x}{\pi_3}\right)^{\pi_4}\right]^{\pi_5} - 1$$

$$\pi_{25} = 1 - \left[1 + \left(\frac{x}{\pi_6}\right)^{\pi_7}\right]^{\pi_8} - \pi_9 e^{\frac{-(x-0.1)^2}{0.005}}$$

$$\theta = \frac{T}{T_C}$$

Table 3.6 Calculation of the Coefficients of saturation pressure

π_0	π_1	π_2	π_3	π_4	π_5	π_6	π_7	π_8	π_9
0.28	4.3	0.6	0.21	5.1	0.49	0.362	-4.75	-0.4	0.03

3.1.4.6 Viscosity of the solution

The viscosity of the solution is calculated based on the concentration and temperature of the solution. As the temperature of the solution increases the viscosity of the solution decreases. Following relation has been proposed for the viscosity of the solution:

$$\eta_{sol}(x, \theta) = \eta_{H2O} e^{\left(\eta_1 x^{3.6} + \eta_2 x + \eta_3 \frac{x}{\theta} + \eta_4 x^2\right)} \tag{3.13}$$

$$x = \frac{x}{(1-x)^{1/0.6}}$$

$$\theta = \frac{T}{228} - 1$$

$$\eta_{H2O} = (A + B\theta^{0.02} + C\theta^{0.04} + D\theta^{0.06} + E\theta^{1.8} + F\theta^8) \tag{3.14}$$

Table 3.7 Coefficient for Dynamic viscosity of solution [36]

η_1	η_2	η_3	η_4
0.090481	1.390262	0.675875	−0.583517

Table 3.8 Coefficients for dynamic viscosity of the subcooled water

A	B	C	D	E	F
1.0261862	12481.702	−19510.923	7065.286	−395.561	143922.996

3.1.5 Properties of the Air

The properties of the air vary with the temperature and hence need to consider while preparing the model. Here we have tried to use the standard values of the air properties being the function of the air temperature. The values of the properties are expanded with an equation of a line and that

equation of a line is fitted with R square value and that equation of line is used in the model to predict the accurate values of the properties throughout the differential element calculation.

3.1.5.1 Specific heat capacity of the Air

The values of the specific heat of air were taken and a equation was plotted to fit those all values and that equation was used in all the model. Below table shows the value of the specific heat at constant pressure and its dependence on the air temperature along with equation used in the model.

$$C_{p,G} = -5 * 10^{-7}T_G^4 + 7 * 10^{-5}T_G^3 - 0.0019T_G^2 + 0.0044T_G^1 + 1006.2$$

Table 3.9 Variation of the Air specific heat capacity with air temperature

T_G	Isobaric specific heat (C_p) (kJ/kg.K)
15.6	1006
26.9	1006
46.9	1007
66.9	1009
86.9	1010

3.1.5.2 Diffusivity of the Air

In Same manner as that of Specific heat the values of the air diffusivity were taken from the standard chart and equation were plotted and used in the model.

$$D_G\left(\frac{m^2}{hr}\right) = 5 * 10^{-7}T_G^2 + 0.0005T_G^1 + 0.0684 \tag{3.15}$$

Table 3.10 Variation of the Air diffusivity with temperature

T_G	Gas Diffusivity in m2/s
30	2.31E-05
50	2.59E-05
75	2.96E-05

43

3.1.5.3 Density of the Air

The density of the air will decrease with the increase in the temperature of the air. Here we have related the standard value of the air density with air temperature and that's how we got an equation which is used in the model. The data is as per following table:

$$\rho_G \left(\frac{kg}{m^3}\right) = 10^{-5}T_G^2 - 0.0044T_G + 1.2877 \qquad (3.16)$$

Table 3.11 Variation of Density of air with the air temp

T_G	Density of air $\frac{kg}{m^3}$
30	1.164
40	1.127
50	1.092
60	1.059
70	1.028
80	0.9994

3.1.5.4 Dynamic viscosity of the Air

The viscosity of air in standard format is known and it is related in the same way as that of other air parameters by creating an equation and using that equation for model. The data is as follows:

Table 3.12 Variation of the Dynamic Viscosity of the air with temperature

T_G	Dynamic Viscosity Pa.hr
30	6.74E-02
40	6.90E-02
50	7.07E-02
60	7.23E-02
70	7.39E-02
80	7.55E-02

$$\mu_G(Pa.hr) = -9*10^{-8}T_G^2 + 0.0002T_G + 0.0623 \qquad (3.17)$$

3.2 Pressure Drop Prediction in Dehumidifier

Air is forced to flow through the packing material. As we know the amount of the air flown has significant impact on the output on the dehumidifier. The more the pressure drop in the packing will require more energy to be supplied to the blowers. Ultimately this adds more cost to the system in the long run decreeing its sustainability. Hence it's really important to add and select proper packing materials for the dehumidifier. The pressure drop is directly related to the size of the blower and hence it's really important to consider the pressure drop in the dehumidifier packing.

Stichilmair et al.,[29] and Castillo et al., [32] and then Gandhidasan et al., [24] has studied the packing for the dehumidification. Here we will be considering the model equations proposed by the Gandhidasan et al., [24] along with that we will be studying the variation of the packing pressure loss. Along with that we are considering the experimental data given by the Koronaki et al.,[67] and we will compare the made model with the existing data given in that paper.

The model applies to both the random and structured packing with little variation by adding corresponding constants of packing for friction factor and liquid drop diameter.

3.2.1 Assumptions for Pressure Drop

- Inlet air velocity is assumed to be without variations or fluctuations
- Thickness of the film formed over the packing is assumed to be constant
- Properties of the air and desiccant are assumed to be constant throughout the packing
- Equivalent diameter is assumed to be constant and is not varying with the liquid holdup

3.2.2 Pressure Drop Equations

The equations are as follows:

equation for the equivalent diameter is:

$$D_P = \frac{6(1-\epsilon)}{a_t}$$

dry bed pressure drop based on the analogy considering the fluidized bed and its given by:

$$\Delta P_d = 0.125 f_0 \frac{\rho_G u_G^2 a_t}{\epsilon^{4.65}}$$

$$f_0 = \frac{C_1}{Re_G} + \frac{C_2}{Re_G^{0.5}} + C_3$$

$$Re_G = \frac{\rho_G D_P u_G}{\mu_G}$$

The static holdup is given by the following formula:

$$h_b = 3.6 \left(\frac{u_L a_t^{0.5}}{g^{0.5}}\right)^{0.66} \left(\frac{\mu_L a_t^{1.5}}{\rho_L g^{0.5}}\right)^{0.25} \left(\frac{\sigma_L a_t^{2.0}}{\rho_L g}\right)^{0.1}$$

When we cross the loading point then the operating liquid holdup is the function of the irrigated or total pressure drop and which can be given by the following equation:

$$h_a = h_b \left[1 + \left(\frac{6\Delta P_{irri}}{\rho_L g}\right)^2\right]$$

$$d_L = C \sqrt{\frac{6\sigma_1}{(\rho_L - \rho_g)g}}$$

Where the C=0.8 for the structured pickings and C =0.4 for the random packing

The effective surface area offered by the liquid particles is given by the following equations:

$$a_L = 6 \frac{h_a}{d_L}$$

The irrigated or the total pressure drop can be calculated by the following equation:

$$\frac{\Delta P_{irri}}{\Delta P_{dry}} = \left(\frac{a_L + a_t}{a_t}\right) \left(\frac{\epsilon}{\epsilon - h_a}\right)^{4.65}$$

flooding pressure drop is:

$$\Delta P_f = \frac{\rho_L g}{2988 h_b} \sqrt{249 h_b \left(\sqrt{X} - 60\epsilon - 558 h_b - 103 d_L D_P\right)}$$

Where flooding coefficient in the above equation can be calculated as follows;

X=3600 ϵ^2+186500 ϵh_b+32300$d_L a_t \epsilon$+191800h_b^2+95030$d_L a_t h_b$+10610$d_L^2 a_t^2$

3.3 Heat and mass transfer Coefficients

From above discussions and equations, we can get the clear view of importance of the heat and mass transfer coefficients and their usage in the moisture FDM model. Hence it is necessary to get

the data of heat and mass transfer coefficients as correct as possible. Ghosh and Chung also presented the data and equations for the coefficients which they got from the dimensional analysis [35]. Here I'm trying to verify the equations given by the Gandhidasan et al.,[24] in his paper. They proposed the equations for the both gas and liquid phase and for both Random and structured packing material. Here we have tried to verify the equation for the structured packing as that's what we are going to consider in the experimental study as well. Here in his paper he has given the heat and mass transfer equations specially for the liquid phase along with the gas phase.

The hydraulic radius of the channel is given by:

$$d = Bh \left[\frac{1}{2S} + \frac{1}{(2S+B)} \right]$$
(3.18)

The void fraction of not given can be calculated by the:

t = sheet thickness, m

$$\epsilon = 1 - \frac{4t}{d}$$
(3.19)

Total packing surface area per unit volume

$$a_t = \frac{4\epsilon}{d}$$
(3.20)

Total holdup is calculated as the:

$$h_{total} = \frac{4c_{total}\delta_{opertating}}{S}$$
(3.21)

$$c_{total} = \frac{29.12[We_L Fr_L]^{0.15} S^{0.359}}{Re_L^{0.2} \epsilon^{0.6} (1 - 0.93 \cos\gamma) \sin\theta^{0.3}}$$
(3.22)

$\theta = Crimp\ angle\ from\ the\ horizontal\ in\ degree$ here it is 60

$\cos\gamma = 0.9\ if\ \sigma < 0.055 \frac{N}{m}$

$\cos\gamma = 5.211 * 10^{-16.835\sigma}\ if\ \sigma \geq 0.055 \frac{N}{m}$

$$\delta_{opertating} = \left[\frac{3\mu_L u_L}{\rho_L \epsilon \sin\theta h_{total} g} \right]^{0.5}$$
(3.23)

Finally, we get

$$h_{total} = \left(\frac{4}{S}c_{total}\right)^{2/3}\left[\frac{3\mu_L u_L}{\rho_L \epsilon \sin\theta h_{total}g}\right]^{1/3} \tag{3.24}$$

From above equation we can calculate the effect ice air and liquid velocity as follows:

$$U_{Ge} = \frac{u_G}{\epsilon \sin\theta(1-h_{total})} \tag{3.25}$$

$$U_{Le} = \frac{u_L}{\epsilon \sin\theta(h_{total})} \tag{3.26}$$

Relative velocity pf the gas to liquid is defined as:

$$U_r = U_{Le} + U_{Ge} \tag{3.27}$$

Here they have given the correlation which is based on the effective velocity of fluid and temperature and concentration.

The heat and mass transfer equation for the gauze type structured packing is as follows for gas side:

$$h_{G,a} = 13.0 U_{Le}^{0.1} U_{Ge}^{0.79} e^{(-0.026 T_G)} \tag{3.28}$$

$$F_{G,a} = 0.55 U_{Le}^{0.1} U_{Ge}^{0.79} e^{(-0.0293 T_G)} \tag{3.29}$$

For lithium chloride-air system they have proposed the following equations:

$$h_{L,a} = 15.1 U_{Le}^{0.4} U_{Ge}^{0.07} e^{(-0.031 T_L)} e^{(-0.003 x)} \tag{3.30}$$

$$F_{L,a} = 8.2 U_{Le}^{0.4} U_{Ge}^{0.07} e^{(-0.038 T_L)} e^{(-0.009 x)} \tag{3.31}$$

From above relations it was found that the heat a mass transfer is strong function of the air and liquid flow rates compared to the temperatures as per the literature.

3.4 Numerical Modeling Platform

Google Colab 3.0 is used for the Numerical modeling. Reason for choosing this platform is as follows:

- It's an online platform for python programming which can be used in multi dimensions.
- Its easily attached with the sharing platform such as GitHub and saves data online.

- All the necessary libraries are available on the Google Colab makes it one of the most updated platform for Python3.0 user base.
- It has its own cloud based google server which is most useful and helps in performing the complex computing.
- Most of it, is free.
- It's quite useful while implementing the Machine learning tools.

Chapter-4

EXPERIMENTAL SETUP

The dehumidifier and regenerator setup exists at the Indian Institute of Technology, Guwahati. This setup has the structured packing of ABS packing material. The auxiliary heater exists which is used in the case of unavailability of proper solar radiation.

4.1 Dehumidifier and Regenerator

These are the major components of the desiccant dehumidification system. In these components heat and mass transfer take place between the desiccant solution and air. Both the heat exchangers are identical in design. They both are insulated by the nitrile foam layer and rubber. Inside the chamber the it is filled with ABS.

Table 4.1 Dehumidifier and Regenerator Design specification [68]

Parameters	Specifications
size	600mm×300mm×150mm
Corrugated angle	45^0
Specific Surface Area	$256 \ m^2/m^3$
Equivalent diameter of flow channel	10 ± 0.5mm
material	ABS
Chamber material	Stainless steel of 3mm thick

Cooling capacity of the system	1 TR
Air mass flow rate	400CFM
Pipe diameter	1 Inch
Centrifugal Blower	2 each of 0.5 HP
Centrifugal pump for solution	2 each of 0.5 HP
Water pump	2 each of 0.5 HP
Cylindrical water tank(insulated)	550mm(diameter)×900mm(length) ×3mm(thick)
Ball valve(to control flow)	Stainless steel 2 in No.
Hose pipe	19.05 mm diameter 50bar capacity
Tubing for cooling Desiccant solution after regeneration	Water cooled Copper tubing of 5 turns 1inch diameter
Shell and tube heat exchanger HX II	To cool the heated desiccant solution with water

4.2 Evacuated Solar tube subset up

The water after exchanging heat is recirculated through the solar ETC for heating it such that it can exchange heat with the desiccant solution in next cycle. The ETC dimensions are given below,

Table 4.2 Solar ETC and its specifications

Specification		Description
Material of glass		3.3 Borosilicate Glass
Length of tube		1800 ± 0.1mm
Inner diameter		47 ± 0.1mm
Outer diameter		58 ± 0.1mm
Absorptive Coating		Three target magnetron sputtering plating of Cu/SS-ALN/ALN (Solar selective coating)
	Emissivity	$\leq 6.5\%$ (80 ± 5^0C)
	Absorptivity(α)	≥ 0.93(AM 1.5)
	transmitivity (τ)	≥ 0.89 (AM 1.5)
Outer diameter of the copper tube		9.53mm
Thickness of the U-tube		0.58mm
Degree of Vacuum		$\leq 5.0 \times 10^{-3}$ Pa
Tilt angle and facing of ETC		26^0 and south

4.3 Considerations from literature survey

Three different fluids (desiccant solution, moist air, process water) are used in the given system. Here we have used the anticorrosive pump to shower the liquid desiccant solution on the corrugated sheets such that when air is flown through it in counter-flow direction the

51

dehumidification or regeneration occurs. The sprayer is made through cutting holes of diameter 4 mm in the pipe. Two blowers are used in the system to force the air and the dimensions of the duct of blower is 25cm×30cm.

- Literature survey has proven that the corrugated structured mesh is preferable and gives good results.
- The flow of air and desiccant is counterblow as it shows better performance.

The pictorial view of the complete setup is shown on the next page [68].

4.4 Sensors and Measuring Instruments

Table 4.3 Technical specifications of measuring instruments

Parameters	Device	Type	Accuracy	Range
Air Flow rate	Anemometer	Testo 490	±0.1 m/s	0–25 m/s
Air/Solution temperature	Temperature sensor	T-type thermocouple	±0.1 ∘C	20–100 ∘C
Air/humidity ratio	Humidity sensor	EQ310CTH	±2% RH	0–100% RH
Solution flow rate	Flow Meter	CM/L-0151526	±2% l/h	60 l/h to 1500 l/h
Density	Hydrometer	Anton-paar 4500 M	±0.005 kg/m3	0 g/cm3 to 3 g/cm3 (Temperature: 0 ∘C–100 ∘C)

4.5 Experimental proposed work

- The Novel desiccant mixture of KCOOH and $ZnBr_2$ will be used in the dehumidifier. The effect of using this binary mixture will be studied.
- The effect of using ABS 250Y Mellapak, Polypropylene packing structure will be studied.
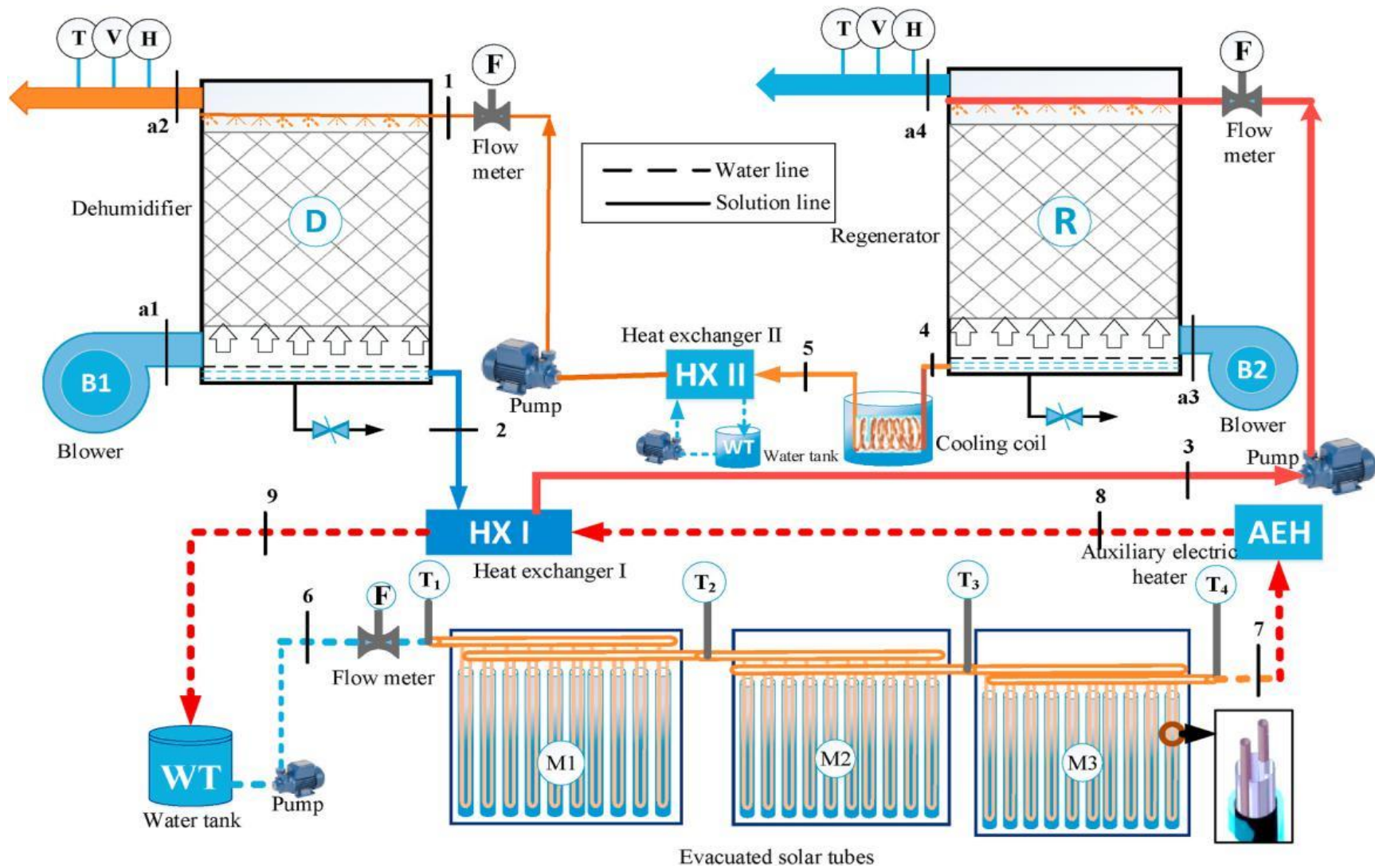- The effect of using different packing surface area and void fraction materials will be studied.

Figure 4.1 Experimental setup with incorporation of solar energy for cooling with ETC [68]

(T: Temperature; H: Humidity; V: Velocity; F: Flowmeter; D: Dehumidifier; B: Blower; P: Pump; HX: Heat exchanger; R: Regenerator; M: Manifolds; AEH: Axillary electric heater; WT: Water heater)

Chapter-5

RESULTS & DISCUSSION

Finite difference model has been adopted for the given numerical study. This study is compared with the experimental data available in the Goswami et al., [26] paper and has been compared. Pressure drop model has been prepared based on the Stichilmair et al., [29] and Gandhidasan et al., [24] study. This pressure drop model is tested with the data available in the paper of the Koronaki et al., [67].Then in last part of the discussion the heat and mass transfer correlations provided by the Al-Farayadhi et al., [25] is tested.

5.1 Finite Difference Model Results

Nelson et al., [26] in his paper has considered the counter flow dehumidifier system. Here they had used polypropylene Hi-flow rings having specific area of 210 m^2/m^3.Here they have given the experimental data and in which they have taken the data set of the average multiple experiments for the data representation. Their input data for the dehumidifier is in the following table. Here we can see that the average error in the humidity prediction, concentration, air outlet temperature, desiccant outlet temperature is less than 7 %, 0.35%, 4%, 4.2% respectively.

Table 5.1 Validation of the FDM Model with paper and model data

Group	Variable								
Inlet Conditions	G	0.89	1.18	1.189	1.19	1.182	1.182	1.192	1.176
	L	6.124	6.227	6.29	5.019	7.42	6.164	6.267	6.206
	L/G	6.880899	5.277119	5.29016	4.217647	6.277496	5.21489	5.25755	5.277211
	Ta	30.1	30.1	35.5	30.1	30.2	29.9	29.9	30
	TL	30.1	30.3	30.3	30.2	30.2	30.1	30.2	30.2
	X	0.346	0.347	0.345	0.344	0.344	0.331	0.338	0.348
	Y	0.018	0.0181	0.0188	0.018	0.0181	0.0179	0.0179	0.0181
Model Predicted Output values	Y	0.011172	0.011831	0.011081	0.012093	0.011794	0.012043	0.011893	0.011822
	X	0.345312	0.346174	0.343975	0.343033	0.343307	0.330254	0.337226	0.34717
	Ta	30.33234	30.40804	34.63225	30.41878	30.42027	30.1925	30.22143	30.30956
	TL	30.87071	31.22915	31.358	31.29483	30.97907	30.96729	31.08873	31.13151
	M$_{condensed}$	0.274906	0.334672	0.415205	0.318021	0.337205	0.313204	0.323935	0.334013
Paper Output Values	Y'	0.0104	0.0108	0.0112	0.0113	0.011	0.0114	0.0112	0.0107
	X'	0.345	0.346	0.337	0.342	0.343	0.33	0.337	0.347
	Ta'	31.3	32.2	32.8	32.2	32	32.4	32.5	32
	TL'	32.3	32.6	32.6	32.7	32.5	32.2	32.6	32.5
	M$_{condensed}$	0.32	0.4	0.42	0.38	0.39	0.36	0.38	0.41
(%) Error	Y(error)%	-7.42493	-9.54269	1.063666	-7.01409	-7.2168	-5.63769	-6.18612	-10.483
	X	0.090412	0.050228	2.069659	0.302072	0.089575	0.077108	0.067078	0.049072
	Ta	3.09158	5.565092	-5.58614	5.531739	4.936659	6.81326	7.010971	5.282636
	TL	4.425038	4.205056	3.809806	4.297144	4.67978	3.828279	4.635806	4.210748
	M$_{condensed}$	14.09199	16.33196	1.141664	16.31016	13.53713	12.99884	14.75404	18.5335

5.2 Performance of Model with Variation of Different Inlet Conditions

The model when tested with different testing conditions by changing one parameter and keeping the other parameter constant the results were logical. The further discussion tells us about the result obtained through the variation of different parameters. Generally, the results are shown in respect to the condensation rate and the dehumidifier effectiveness. The initial conditions assumed are solution flow rate as 6.29 kg/m^2.s ,30.3℃, 35.5℃ solution, air temperature and 34.5% concentration with 5.29 flow ratio and 0.0188 kg/kg of dry air, as inlet specific humidity.

5.2.1 Effect of Air Flow Rate

It is evident from the figure that, with increase in the air flow rate, condensation rate increases.
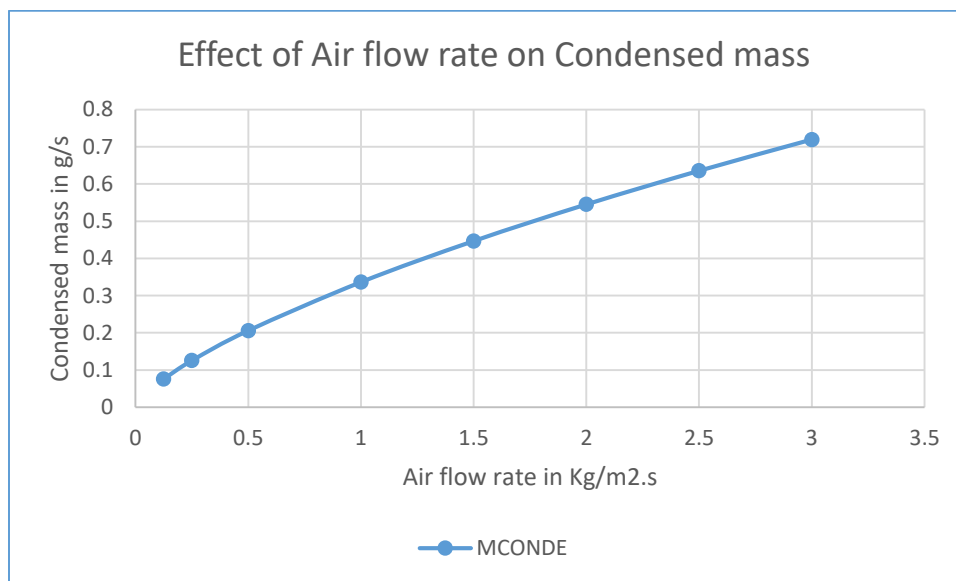

Figure 5.1 variation of the Material removal rate with air flow rate

The higher flow rate of the air removes the air more rapidly form the packing interface where absorption take place. With this the humidity gradient between the interface and the air is reduced which results in increases in the potential for the mass transfer. As the more the humidity the more will be the vapor pressure of the water in the air so directly the potential driving for the mass transfer will be more. With increase in the mass flow rate the, velocity of the air is increased and it also decreases the time the solution and air interact and hence because of that the lesser amount

of the humidity is removed even if it has more potential. Hence this decreases the humidity effectiveness with the air flow rate.
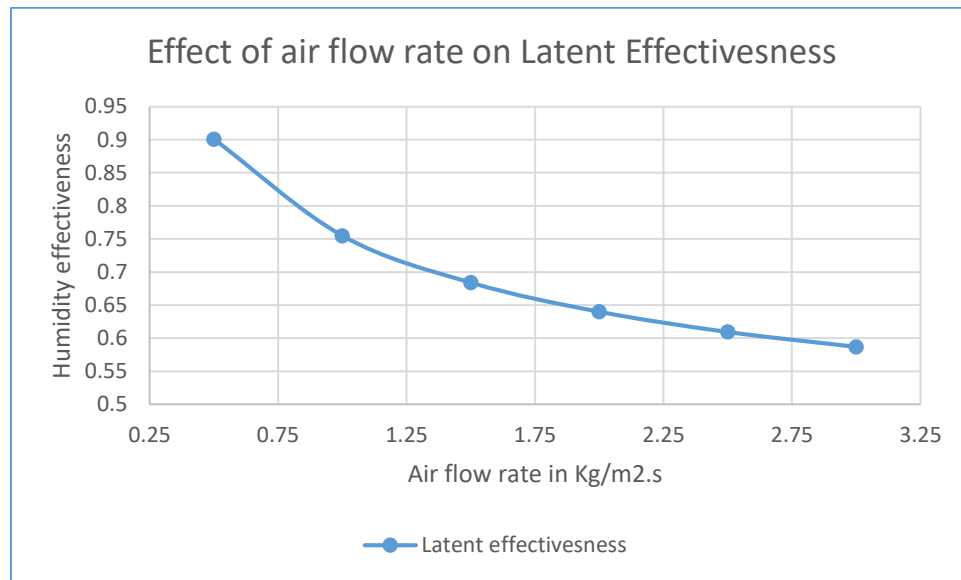

Figure 5.2 Variation of Humidity effectiveness with inlet air flow rate

5.2.2 Effect of the Desiccant Temperature

With increase in the desiccant temperature the vapor pressure of the water at the interface increases. This increase in vapor pressure at the interface reduces the mass transfer potential decreasing the overall mass transfer characteristics as the temp of inlet air is kept constant. With increase in the desiccant temperature the saturated vapor humidity at the desiccant temperature will increase. This leads to the decrease in the denominator term which increases the overall effectiveness of the dehumidifier as the other parameters such as the concentration are kept constant.
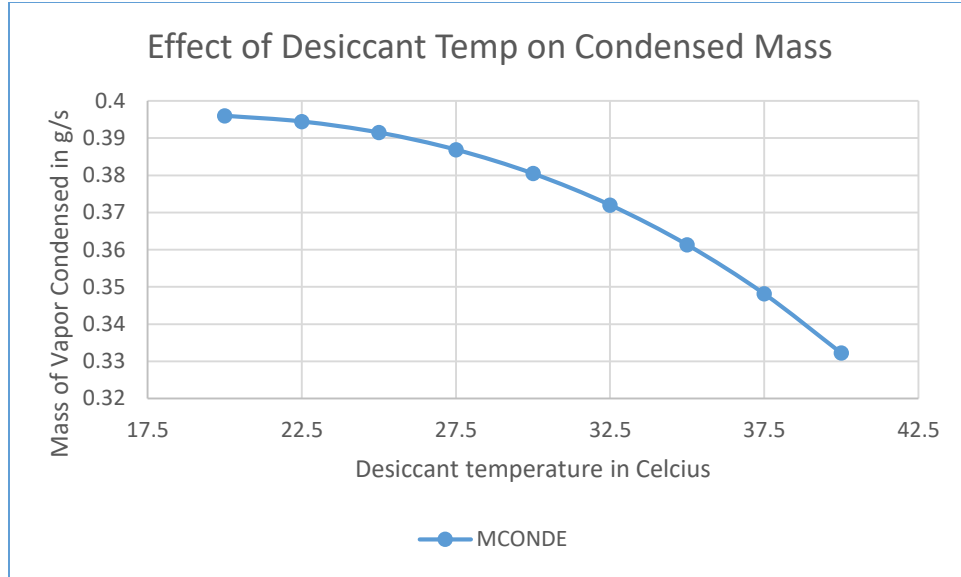
Figure 5.3 variation of the mass of vapor condensed with the inlet Desiccant temperature
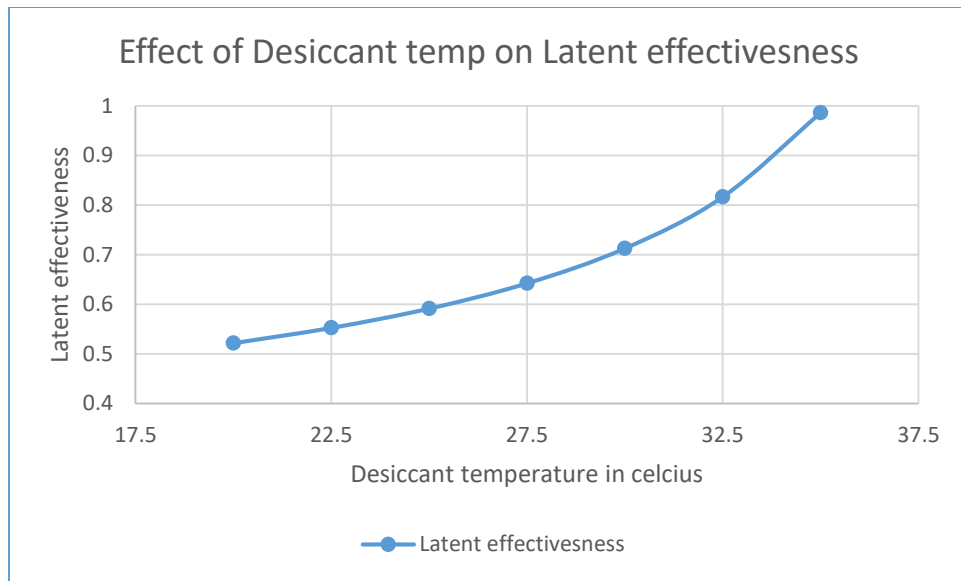

Figure 5.4 Variation of the Latent Effectiveness with Desiccant Temperature

5.2.3 Effect of the Concentration

Water condensation rate will increase with the increase in the concentration. As the concentration will increase the potential for the mass transfer and will lead to increases in more absorption; due to lowering the overall pressure at the interface. Hence the difference between the water vapor pressure will increase.
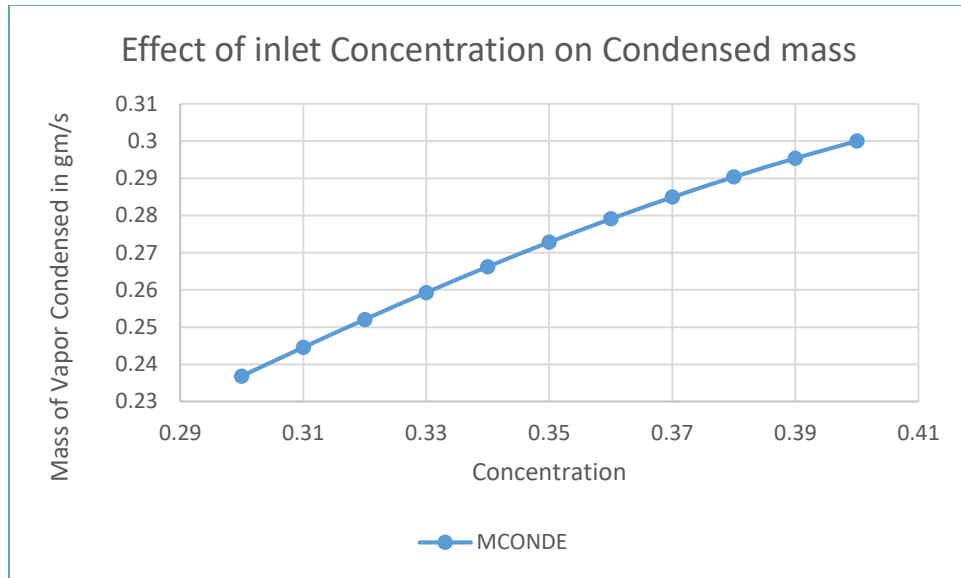
Figure 5.5 variation of the mass of vapor condensed with the inlet Desiccant Concentration

The temperature remains constant but the overall equilibrium humidity will increase and this lower the effectiveness of the dehumidifier.

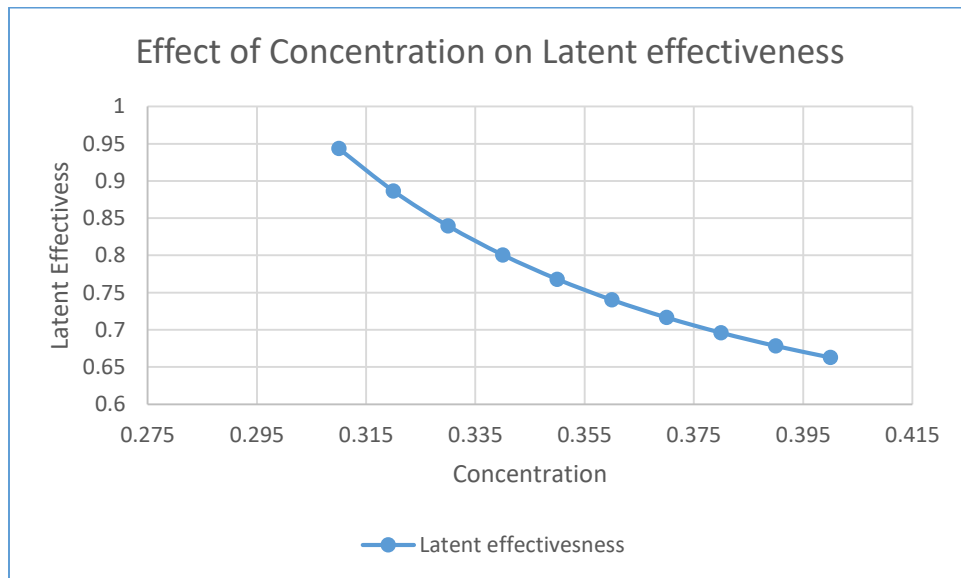Figure 5.6 variation of the latent effectiveness with the inlet Desiccant Concentration

5.2.4 Effect of the Solution Flow Rate

As the effect of increasing the flow rate is as such to increase the velocity of the liquid. This increases the potential for the mass transfer as it can be seen from the mass transfer equations. But this effect is stabilized after the sufficient wetting of the packing area.
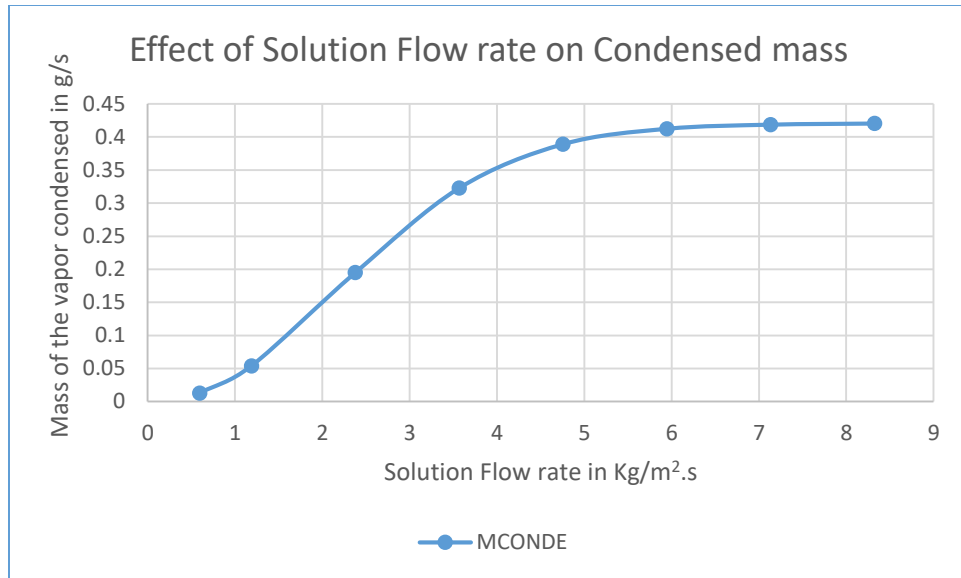
Figure 5.7 Variation of the mass of the vapor condensed with the solution flow rate
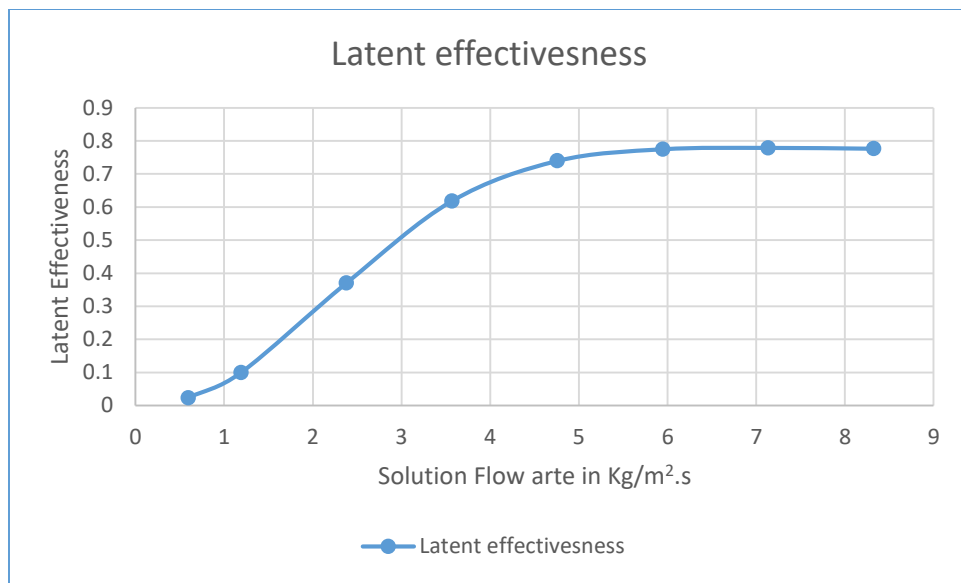
Figure 5.8 Variation of the Latent effectiveness with the Solution flow rate

As the flow rate increases this leads to increase in the latent effectiveness in starting as the more potential is available for the mass transfer and it allows for the humidity transfer. But after certain value of the flow rate the effect of increasing mass flow rate is mere constant as the packing is sufficiently wet and more amount of liquid adds to nothing but to pumping cost. Hence the effectiveness is nearly constant after certain value.

5.3 Pressure Drop in Dehumidifier

Koronaki et al.,[67] in his paper has given and solved for the packing and pressure loss. The following table compares the data from his paper and data from the model made to predict the pressure drop when the air velocity increased or the air flow rate is increased. It is obvious that as the air flow rate will increase it will lead to increase in the liquid holdup decreasing the flow area and hence reducing the actual void space. This enhances the air obstruction and hence the pressure drop increases with the increase in the air flow rate.

Table 5.2 Validation of data from the Koronaki et al. [67] paper and Model data

air mass flow rate (Kg/s)	Pressure drop from Paper(Pa/m)	Dry pressure from Model (Pa/m)	dynamic holdup From model	Total pressure drop from model (Pa/m)	flooding pressure drop from model (Pa/m)	error(%)
0.006118	3.626845	3.289808	0.010003	3.607396	4728.398	0.536267
0.010115	9.48672	8.433531	0.010004	9.247693	4728.398	2.519596
0.020309	35.5869	31.76862	0.010006	34.8364	4728.398	2.108915
0.040778	135.519	121.9503	0.010047	133.7769	4728.398	1.285528
0.061808	303.5293	273.9796	0.010225	301.0428	4728.398	0.819218
0.08044	511.3731	458.5166	0.01063	505.6852	4728.398	1.112278
0.101152	787.8438	718.3438	0.011568	799.1023	4728.398	-1.42902

From above we can state that the value for the total pressure drop in Koronaki et al., [67] paper and model made here gives the prediction which matches to the most. From above it can be said that the total pressure drop increases with the increase in the air flow rate.
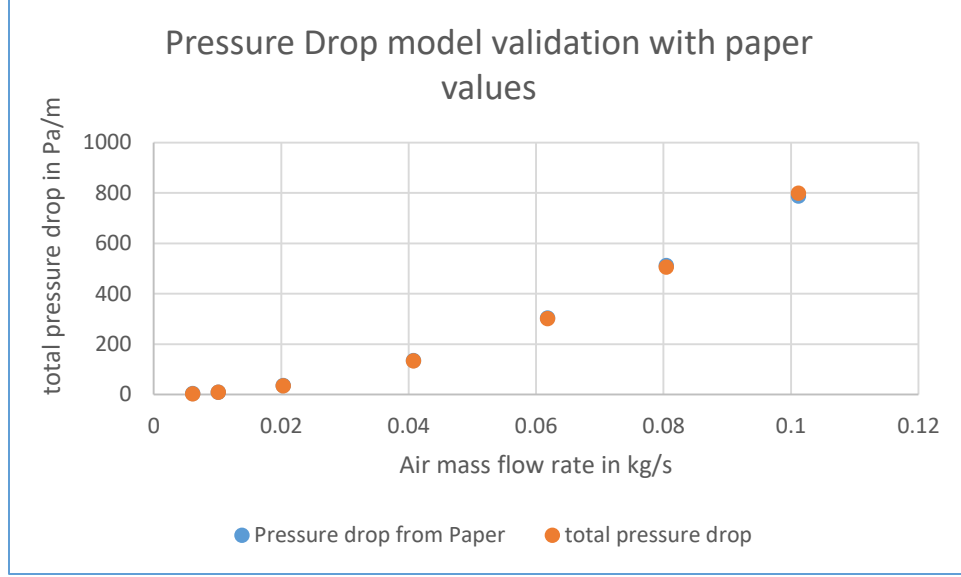
Figure 5.9 Pressure Drop Model Validation with Koronaki et al. [67] Paper Values

5.4 Heat and Mass Transfer Coefficients

The coefficients of mass and heat transfer given by the Gandhidasan et al., [25] in his paper utilizes the effective velocity of liquid and gas phase. This equation also takes into account the temperature of the air, desiccant and concentration. This equation has been tested with the conditions given in the paper. Here we have tried to reproduce the results for the both liquid and gas phase constants. The equations are as follows:

The heat and mass transfer equation for the gauze type structured packing is as follows for gas side:

$$h_{G,a} = 13.0 U_{Le}{}^{0.1} U_{Ge}{}^{0.79} e^{(-0.026 T_G)}$$

$$F_{G,a} = 0.55 U_{Le}{}^{0.1} U_{Ge}{}^{0.79} e^{(-0.0293 T_G)}$$

For lithium chloride-air system they have proposed the following equations:

$$h_{L,a} = 15.1 U_{Le}{}^{0.4} U_{Ge}{}^{0.07} e^{(-0.031 T_L)} e^{(-0.003x)}$$

$$F_{L,a} = 8.2 U_{Le}{}^{0.4} U_{Ge}{}^{0.07} e^{(-0.038 T_L)} e^{(-0.009x)}$$

5.4.1 Volumetric Heat transfer coefficient Vs Effective air velocity

The volumetric heat transfer coefficients showed little variation form the original equation even though the all the values were taken from the paper. The average error in predicting the volumetric heat transfer coefficient was around 20% with the variation of the effective air velocity (0.85 m/s-1.45 m/s). Below graph shows the following variation in the model values and the paper values. Increase in the air velocity will definitely improve the heat transfer coefficient in forced process. The lesser contact time gives more potential to increase the volumetric mass transfer potential.
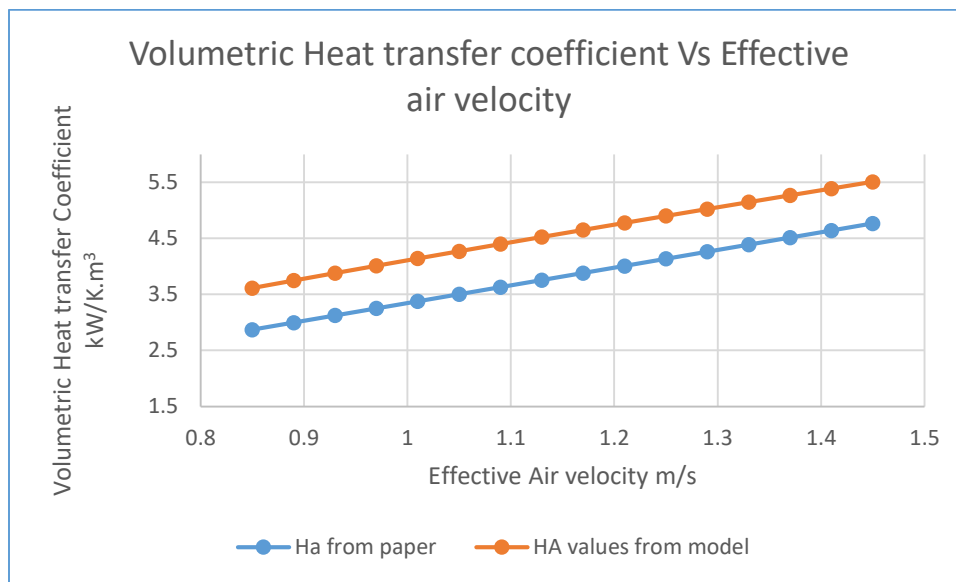

Figure 5.10 variation of Volumetric Heat transfer coefficient with Effective air velocity [25]

5.4.2 Variation of Air Volumetric Mass Transfer Coefficient with Effective Air Velocity

Here the air temperature was kept around the 25 ℃ and the effective velocity of the liquid was kept around 0.0066m/s and the air velocity was varied from the (0.85-1.45 m/s). The average error in predicting the volumetric mass transfer coefficient was found to be around 21.5%. The concentration of the LiCl solution was around 40%. The variation in the predicted and paper values is shown in the graph. As the air velocity increases so the slope of the variation in the pressure across the interface increases without utilizing the full potential of mas transfer which leads to increase in the more mass transfer. The interface air will be renewed will supply new air every time giving lesser time which corresponds to high starting potential near surface interface leading to increase in the mass transfer.
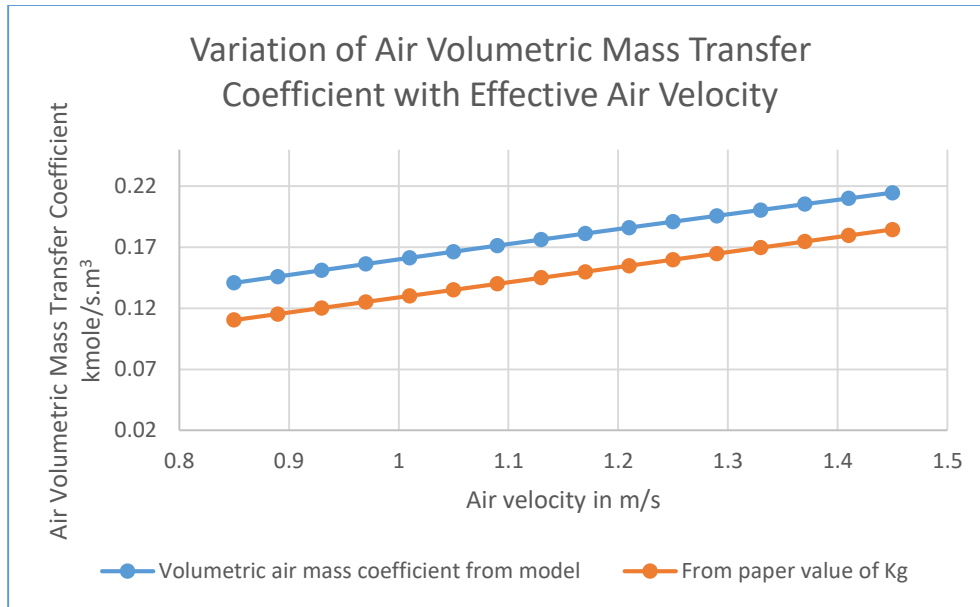
63

Figure 5.11 Variation of Air Volumetric Mass Transfer Coefficient with Effective Air Velocity [25]

5.4.3 Variation of Liquid Volumetric Mass Transfer Coefficient with Effective Liquid Velocity

Here the LiCl solution with 40% concentration, 10.5m/s effective air velocity was kept constant. The effective liquid velocity was varied from the 0.03 to 0.27 m/s and the variation of the volumetric mass transfer coefficient was studied. The results of the paper and the found data showed great similarities. The average error in predicting the coefficient was less than 0.3%. The variation of the Volumetric mass transfer coefficient for the liquid with liquid effective velocity is shown in the below graph. It can be stated that the more the velocity of the liquid more the mass transfer potential as the potential will be utilized to less extent and will be renewed and hence allows to increase the mass transfer coefficient to increase.
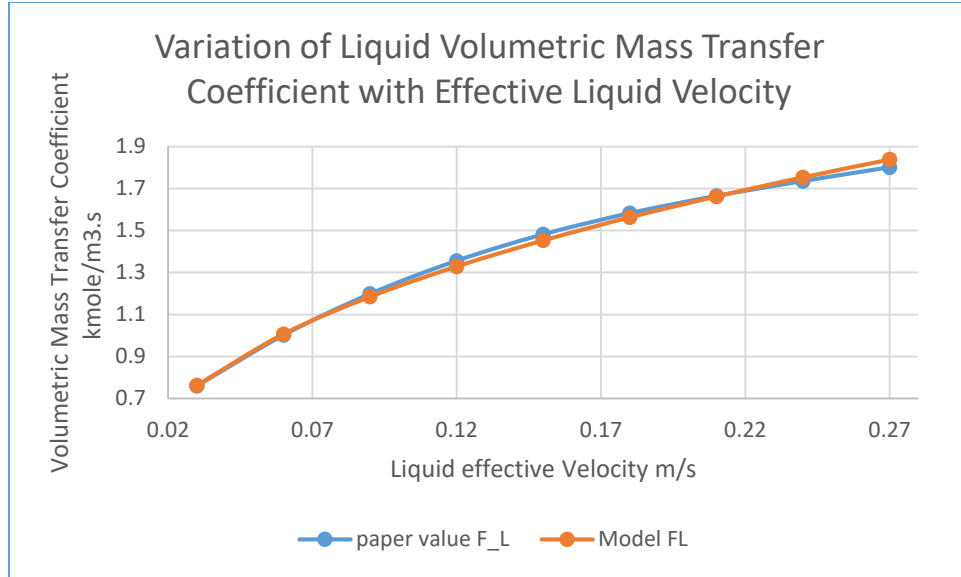
Figure 5.12 Variation of Liquid Volumetric Mass Transfer Coefficient with Effective Liquid Velocity[25]

5.4.4 Variation of Liquid Volumetric Mass Transfer Coefficient with Liquid Concentration

The volumetric mass transfer coefficient increases slightly with the increase in the concentration of the solution. As the concentration increases it leads to increasing the potential for the mass transfer by decreasing the interface surface vapor pressure. But the effect of the increase in the value of the Volumetric mass transfer coefficient is less compared to the effect of the flow rates. The average error in calculation of the volumetric mass transfer coefficient was around 0.3%. Below graph shows the variation of the predicted and paper value for the volumetric mass transfer coefficient with solution concentration.

Figure 5.13 Variation of Liquid Volumetric Mass Transfer Coefficient with Liquid Concentration [25]

5.4.5 Variation of Liquid Volumetric Mass Transfer Coefficient with Liquid Desiccant temperature

As the desiccant solution temperature increase it leads to weakening of the bond with water. This increase the pressure above the interface and hence the vapor pressure difference between the interface and air decreases which leads to decrease in the potential for the mass transfer. This can be clearly seen in the following graph where the volumetric mass transfer coefficient is decreasing with the increasing the desiccant temperature. The average error in the finding was around 0.8%.
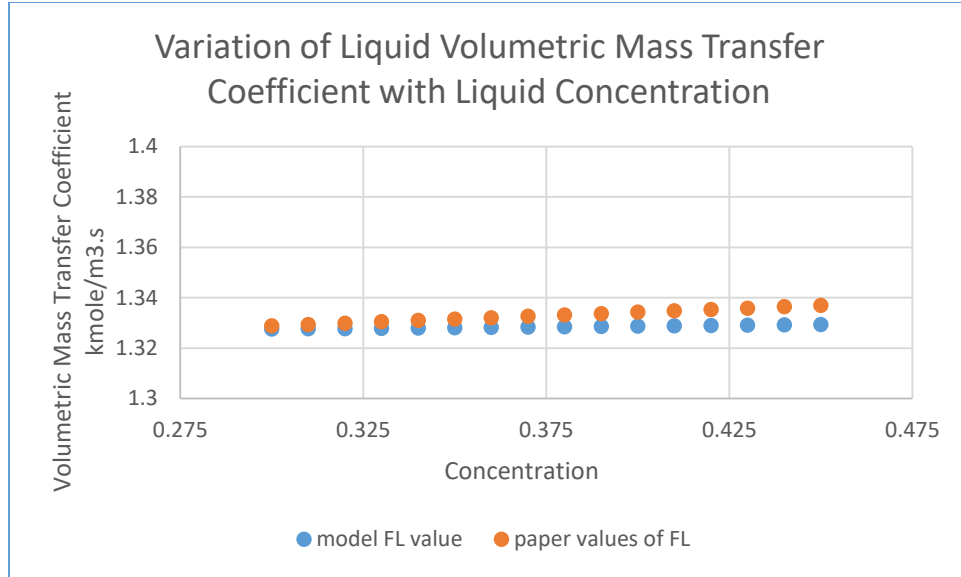
Figure 5.14 Variation of Liquid Volumetric Mass Transfer Coefficient with Liquid Desiccant temperature [25]

5.4.6 Variation of Liquid Volumetric Heat Transfer Coefficient with Liquid Desiccant Temperature

The volumetric heat transfer coefficient is weak function of the desiccant temperature as it can be seen from the below graph. While predicting the volumetric heat transfer coefficient the effective air, liquid velocities were kept to be constant around 10.5 m/s, 0.12 m/s and concentration was kept to 40%. The average error in predicting the volumetric heat transfer coefficient was around 5%. the model and paper comparison is shown in the following graph.
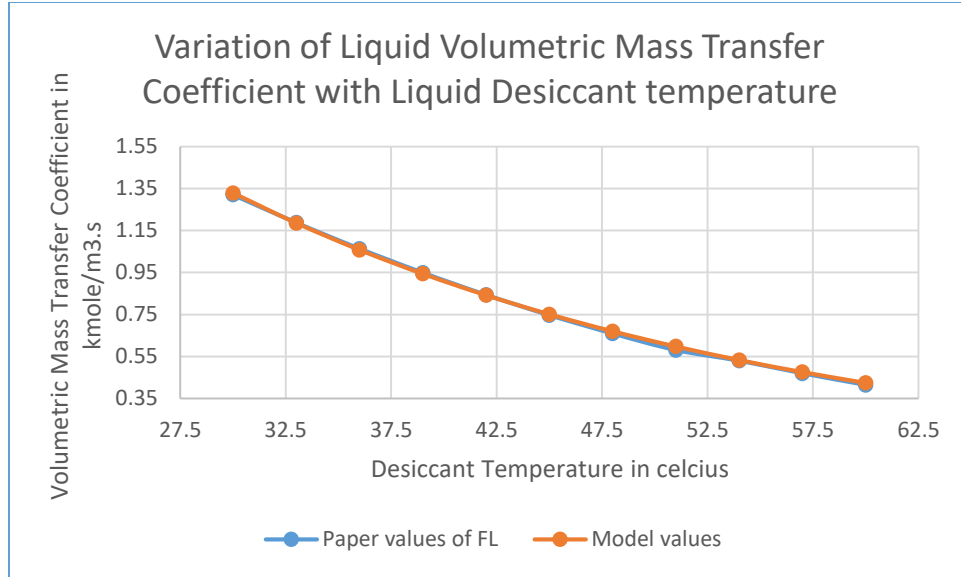
Figure 5.15 Variation of Liquid Volumetric Heat Transfer Coefficient with Liquid Desiccant Temperature [25]

5.4.7 Variation of Liquid Volumetric Heat Transfer Coefficient with Effective Liquid Velocity

Increasing the Velocity of the liquid increases the volumetric heat transfer coefficient. Here they have considered the variation of the liquid velocity to be in the range of 0.03 to 0.27 m/while calculating the effect the air effective velocity was kept constant to be around 10.5 m/s and the desiccant temperature was 30℃ with 40% concentration of LiCl solution. The below graph shows the variation of the volumetric heat transfer coefficient with effective liquid velocity. The average error in the findings were around the 1.5%.
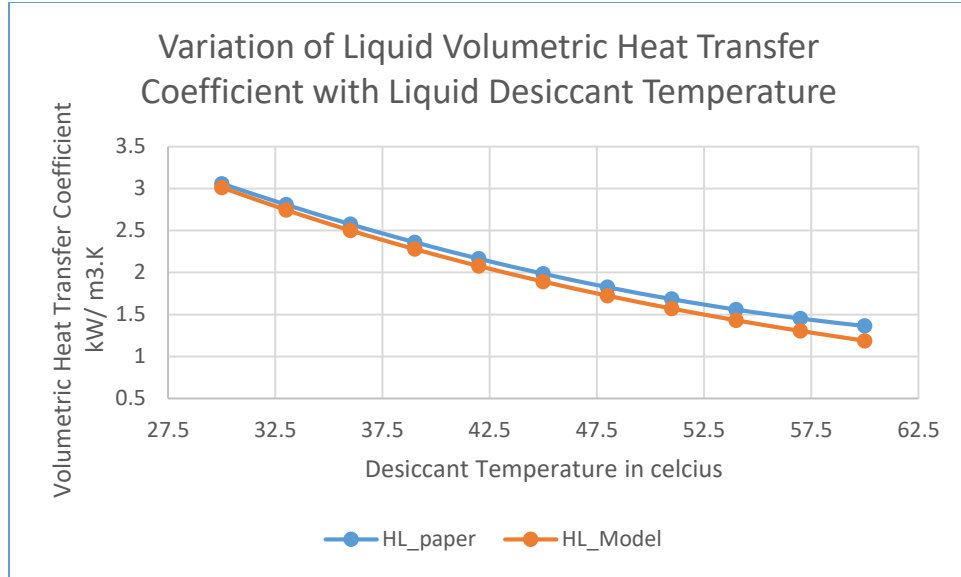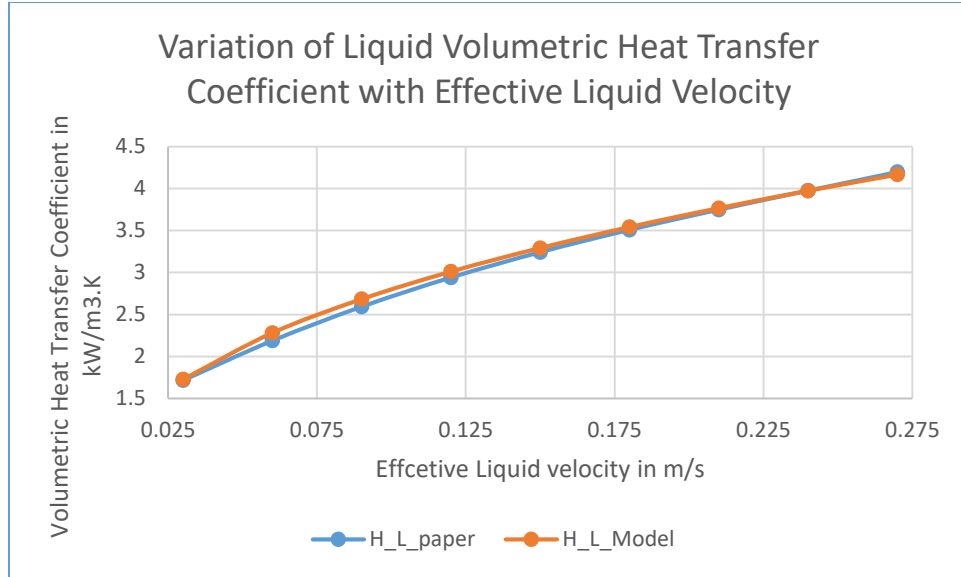
Figure 5.16 Variation of Liquid Volumetric Heat Transfer Coefficient with Effective Liquid Velocity [25]

5.4.8 Variation of Liquid Volumetric Heat Transfer Coefficient with Solution Concentration

The effect of variation of concentration is negligible on volumetric heat transfer coefficient. Here they have considered the air and liquid effective velocities to be around 10.5 and 0.12 with 30℃ concentration. The average error in the findings were around 0.12%. the below graph shows the volumetric heat transfer coefficient variation with solution concentration.
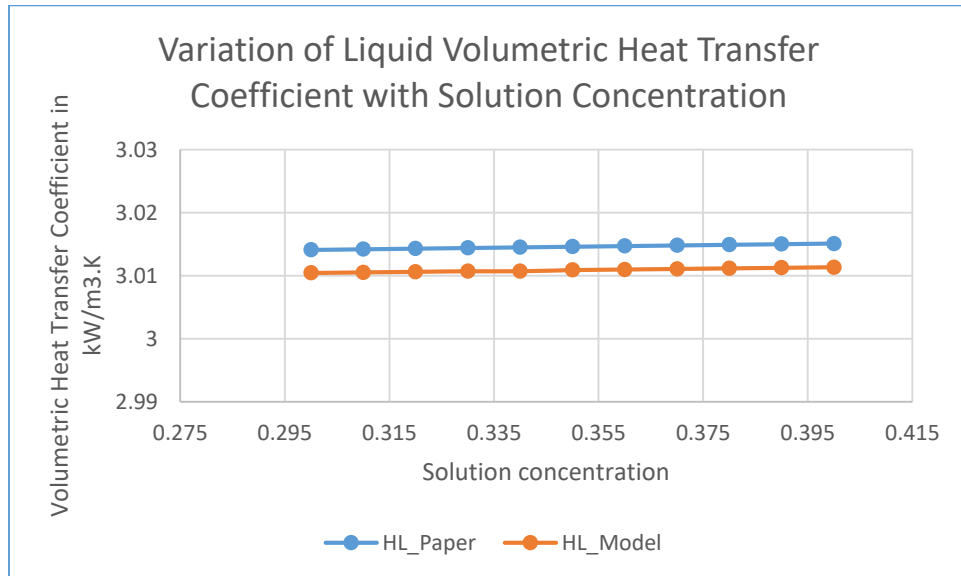

Figure 5.17 Variation of Liquid Volumetric Heat Transfer Coefficient with Solution Concentration [25]

69

CONCLUSION

Followings key conclusions can be drawn from the study:

- Packed bed dehumidifier has been studied here with the help of Finite difference method. The average error in the outlet specific humidity, concentration, air outlet temperature, desiccant outlet temperature is less than 7 %, 0.35%, 4%, 4.2% respectively. These values are less than the allowable error given in the research paper.

- Pressure drop was calculated for polypropylene structured packing for the LiCl desiccant solution. The calculated results have been compared with the literature data. The error in the pressure drop prediction was less than 2.5%.

- The calculation of pressure drop per unit length for Mellapak 250Y was lowest for $CaCl_2$ desiccant solution.

- The heat and mass transfer coefficients are the most important coefficients which drive the humidity equations. The equations for the coefficients were found and were calculated for the data given in the literature and satisfactory results were shown with air heat and mass transfer coefficients. The liquid heat and mass transfer coefficients were found to be matching to the literature data with error less than 2% in some cases.

FUTURE WORK

Following points show the work that will be addressed in the future:

- Numerical Model will be expanded for the KCOOH+ZnBr$_2$ binary solution.

- Experimental work will be done on KCOOH+ZnBr$_2$ binary solution.

- To study the effect of different Structured packing on dehumidifier performance.

REFERENCES

[1]   T. E. and R. I. (TERI); N. R. D. C. (NRDC); I. for G. & S. Development, "Improving Air Conditioners in India," 2018. [Online]. Available: https://www.teriin.org/sites/default/files/2018-04/improving-air-conditioners-in-india.pdf.

[2]   Z. Yang *et al.*, "Analysis of Lower GWP and Flammable Alternative Refrigerants," *Int. J. Refrig.*, 2021, doi: 10.1016/j.ijrefrig.2021.01.022.

[3]   V. Nair, "HFO refrigerants: A review of present status and future prospects.," *Int. J. Refrig.*, vol. 122, pp. 156–170, 2021, doi: 10.1016/j.ijrefrig.2020.10.039.

[4]   UNFCC, "Kigali amendment to the montreal Protocol : A Crucial Step in the Fight Against Catastrophic Climate Change," *EIA Brief. to 22nd Conf. Parties to United Nations Framew. Conv. Clim. Chang.*, no. October, pp. 1–4, 2016, [Online]. Available: https://eia-international.org/wp-content/uploads/EIA-Kigali-Amendment-to-the-Montreal-Protocol-FINAL.pdf.

[5]   B. Saleh, "Energy and exergy analysis of an integrated organic Rankine cycle-vapor compression refrigeration system," *Appl. Therm. Eng.*, vol. 141, no. May, pp. 697–710, 2018, doi: 10.1016/j.applthermaleng.2018.06.018.

[6]   L. Crofoot, "Experimental evaluation and modeling of a solar liquid desiccant air conditioner," 2012.

[7]   S. Y. Ahmed, P. Gandhidasan, and A. A. Al-Farayedhi, "Thermodynamic analysis of liquid desiccants," *Sol. Energy*, vol. 62, no. 1, pp. 11–18, 1998, doi: 10.1016/S0038-092X(97)00087-X.

[8]   D. B. Jani, M. Mishra, and P. K. Sahoo, "A critical review on application of solar energy as renewable regeneration heat source in solid desiccant – vapor compression hybrid cooling system," *J. Build. Eng.*, vol. 18, no. January, pp. 107–124, 2018, doi: 10.1016/j.jobe.2018.03.012.

[9]   J. De Liang, B. H. Huang, Y. C. Chiang, and S. L. Chen, "Experimental investigation of a

liquid desiccant dehumidification system integrated with shallow geothermal energy," *Energy*, vol. 191, p. 116452, 2020, doi: 10.1016/j.energy.2019.116452.

[10] I. Sarbu and C. Sebarchievici, "Review of solar refrigeration and cooling systems," *Energy Build.*, vol. 67, pp. 286–297, 2013, doi: 10.1016/j.enbuild.2013.08.022.

[11] A. Giampieri, Z. Ma, A. Smallbone, and A. P. Roskilly, "Thermodynamics and economics of liquid desiccants for heating, ventilation and air-conditioning – An overview," *Appl. Energy*, vol. 220, no. December 2017, pp. 455–479, 2018, doi: 10.1016/j.apenergy.2018.03.112.

[12] A. Gurubalan, M. P. Maiya, and P. J. Geoghegan, "A comprehensive review of liquid desiccant air conditioning system," *Appl. Energy*, vol. 254, no. March, p. 113673, 2019, doi: 10.1016/j.apenergy.2019.113673.

[13] M. Salikandi, B. Ranjbar, E. Shirkhan, S. Shanmuga Priya, I. Thirunavukkarasu, and K. Sudhakar, "Recent trends in liquid desiccant materials and cooling systems: Application, performance and regeneration characteristics," *J. Build. Eng.*, vol. 33, no. June 2020, p. 101579, 2021, doi: 10.1016/j.jobe.2020.101579.

[14] H. X. Fu and X. H. Liu, "Review of the impact of liquid desiccant dehumidification on indoor air quality," *Build. Environ.*, vol. 116, pp. 158–172, 2017, doi: 10.1016/j.buildenv.2017.02.014.

[15] I. Girnik, T. Yang, L. Gordeeva, W. Wang, T. Ge, and Y. Aristov, "New adsorption method for moisture and heat exchange in ventilation systems in cold countries: Concept and mathematical simulation," *Energies*, vol. 16, no. 3, 2020, doi: 10.3390/en13061386.

[16] M. M. Tokarev, L. G. Gordeeva, A. D. Grekova, and Y. I. Aristov, "Adsorption cycle 'heat from cold' for upgrading the ambient heat: The testing a lab-scale prototype with the composite sorbent CaClBr/silica," *Appl. Energy*, vol. 211, no. October 2017, pp. 136–145, 2018, doi: 10.1016/j.apenergy.2017.11.015.

[17] Y. K. Seo *et al.*, "Energy-efficient dehumidification over hierachically porous metal-organic frameworks as advanced water adsorbents," *Adv. Mater.*, vol. 24, no. 6, pp. 806–810, 2012, doi: 10.1002/adma.201104084.

[18] Y. Fang, W. Yao, J. Guo, and X. Gao, "Characterization and performance of novel modified silica gel/molecular sieve composite," *Int. J. Low-Carbon Technol.*, vol. 7, no. 4, pp. 271–274, 2012, doi: 10.1093/ijlct/cts045.

[19] A. Dąbrowski, "Adsorption - From theory to practice," *Adv. Colloid Interface Sci.*, vol. 93, no. 1–3, pp. 135–224, 2001, doi: 10.1016/S0001-8686(00)00082-8.

[20] P. M. Gundry and F. C. Tompkins, "Chemisorption of gases on metals," *Q. Rev. Chem. Soc.*, vol. 14, no. 3, pp. 257–291, 1960, doi: 10.1039/qr9601400257.

[21] Y. J. Dai and H. F. Zhang, "Numerical simulation and theoretical analysis of heat and mass transfer in a cross flow liquid desiccant air dehumidifier packed with honeycomb paper," *Energy Convers. Manag.*, vol. 45, no. 9–10, pp. 1343–1356, 2004, doi: 10.1016/j.enconman.2003.09.006.

[22] M. M. Bassuoni, "An experimental study of structured packing dehumidifier/regenerator operating with liquid desiccant," *Energy*, vol. 36, no. 5, pp. 2628–2638, 2011, doi: 10.1016/j.energy.2011.02.004.

[23] R. E. Treybal, *Mass Transfer Operations*. 1981.

[24] P. Gandhidasan, "Prediction of pressure drop in a packed bed dehumidifier operating with liquid desiccant," *Appl. Therm. Eng.*, vol. 22, no. 10, pp. 1117–1127, 2002, doi: 10.1016/S1359-4311(02)00031-5.

[25] A. A. Al-Farayedhi, P. Gandhidasan, and M. A. Al-Mutairi, "Evaluation of heat and mass transfer coefficients in a gauze-type structured packing air dehumidifier operating with liquid desiccant," 2002. [Online]. Available: www.elsevier.com/locate/ijrefrig.

[26] N. Fumo and D. Y. Goswami, "Study of an aqueous lithium chloride desiccant system: Air dehumidification and desiccant regeneration," *Sol. Energy*, vol. 72, no. 4, pp. 351–361, 2002, doi: 10.1016/S0038-092X(02)00013-0.

[27] Ž. Olujić, B. Kaibel, H. Jansen, T. Rietfort, E. Zich, and G. Frey, "Distillation column internals/configurations for process intensification," *Chem. Biochem. Eng. Q.*, vol. 17, no. 4, pp. 301–309, 2003.

[28] T. J. Montz, "Your partner in chemical engineering," Hilden, Germany. [Online]. Available: https://irp-cdn.multiscreensite.com/3601d62c/files/uploaded/Montz_Catalog_en.pdf.

[29] J. Stichlmair, J. L. Bravo, and J. R. Fair, "General model for prediction of pressure drop and capacity of countercurrent gas/liquid packed columns," *Gas Sep. Purif.*, vol. 3, no. 1, pp. 19–28, 1989, doi: 10.1016/0950-4214(89)80016-7.

[30] S. Shojaee, S. H. Hosseini, A. Rafati, and G. Ahmadi, "Prediction of the effective area in structured packings by computational fluid dynamics," *Ind. Eng. Chem. Res.*, vol. 50, no. 18, pp. 10833–10842, 2011, doi: 10.1021/ie200088d.

[31] U. S. P. R. Arachchige and M. C. Melaaen, "Selection of Packing Material for Gas Absorption," *Eur. J. Sci. Res.*, vol. 87, no. 1, pp. 117–126, 2012, [Online]. Available: http://www.europeanjournalofscientificresearch.com.

[32] J. R. Ortiz-Del Castillo, G. Guerrero-Medina, J. Lopez-Toledo, and J. A. Rocha, "Design of steam-stripping columns for removal of volatile organic compounds from water using random and structured packings," *Ind. Eng. Chem. Res.*, vol. 39, no. 3, pp. 731–739, 2000, doi: 10.1021/ie990432m.

[33] M. Bhowmik, P. Muthukumar, and R. Anandalakshmi, "Experimental investigation on structured packed bed liquid desiccant dehumidifier: An optimal mixture design of experiments strategy," *Int. J. Refrig.*, vol. 122, pp. 232–244, 2021, doi: 10.1016/j.ijrefrig.2020.11.006.

[34] "WIRE GAUZE PACKING BX HC ® wire gauze packing," 2018. https://www.sulzer.com/-/media/files/products/separation-technology/liquid_liquid_extraction/brochures/structured_packings.ashx.

[35] T. W. Chung, T. K. Ghosh, and A. L. Hines, "Comparison between Random and Structured Packings for Dehumidification of Air by Lithium Chloride Solutions in a Packed Column and Their Heat and Mass Transfer Correlations," *Ind. Eng. Chem. Res.*, vol. 35, no. 1, pp. 192–198, 1996, doi: 10.1021/ie940652u.

[36] M. R. Conde-Petit, "Aqueous solutions of lithium and calcium chlorides: – Property formulations for use in air conditioning equipment design," *M. Conde Eng.*, 2009.

[37] J. A. Rocha, J. L. Bravo, and J. R. Fair, "Distillation Columns Containing Structured Packings : A Comprehensive Model for Their Performance . 2 . Mass-Transfer Model," pp. 1660–1667, 1996.

[38] Y. Luo, H. Yang, L. Lu, and R. Qi, "A review of the mathematical models for predicting the heat and mass transfer process in the liquid desiccant dehumidifier," *Renew. Sustain. Energy Rev.*, vol. 31, pp. 587–599, 2014, doi: 10.1016/j.rser.2013.12.009.

[39] H. M. Factor and G. Grossman, "A packed bed dehumidifier/regenerator for solar air conditioning with liquid desiccants," vol. 24, no. 1, 1980.

[40] D. Y. Goswami and N. Fumo, "Study of an aqueous lithium chloride desiccant system: air dehumidification and desiccant regeneration," *Sol. Energy*, vol. 72, no. 4, pp. 351–361, 2002.

[41] V. Oberg and D. Y. Goswami, "Experimental Study of the Heat and Mass Transfer in a Packed Bed Liquid Desiccant Air Dehumidifier," no. November 1998, pp. 289–297, 2016.

[42] C. F. Keftleborough, "Analysis of Heat and Mass Transfer Between a Desiccant-Air System in a Packed Tower," vol. 1, no. May 1987, 2015.

[43] H. Pahlavanzadeh and P. Nooriasl, "Experimental and Theoretical Study of Liquid Desiccant Dehumidification System by Using the Effectiveness Model," *J. Therm. Sci. Eng. Appl.*, vol. 4, no. 1, pp. 1–9, 2012, doi: 10.1115/1.4005210.

[44] A. Ertas, E. E. Anderson, and I. Kiris, "Properties of a new liquid desiccant solution-Lithium chloride and calcium chloride mixture," *Sol. Energy*, vol. 49, no. 3, pp. 205–212, 1992, doi: 10.1016/0038-092X(92)90073-J.

[45] S. Bouzenada, A. N. Kaabi, L. Frainkin, T. Salmon, and A. Léonard, "Experimental Comparative Study on Lithium Chloride and Calcium Chloride Desiccants," *Procedia Comput. Sci.*, vol. 83, pp. 718–725, 2016, doi: 10.1016/j.procs.2016.04.159.

[46] N. Fumo and D. Y. Goswami, "STUDY OF AN AQUEOUS LITHIUM CHLORIDE DESICCANT SYSTEM : AIR DEHUMIDIFICATION AND DESICCANT REGENERATION," vol. 72, no. 4, pp. 351–361, 2002.

[47] Y. He, N. Gao, and G. Chen, "Isobaric specific heat capacity of typical lithium chloride liquid desiccants using scanning calorimetry," *J. Chem. Thermodyn.*, vol. 70, pp. 81–87, 2014, doi: 10.1016/j.jct.2013.10.028.

[48] S. Sabek, K. Ben Nasr, F. Tiss, R. Chouikh, and A. Guizani, "Performance investigation of desiccant liquid air membrane energy exchanger: Air and lithium chloride effects," *Int. J. Refrig.*, vol. 80, pp. 145–157, 2017, doi: 10.1016/j.ijrefrig.2017.04.027.

[49] H. C. Duong, F. I. Hai, A. Al-Jubainawi, Z. Ma, T. He, and L. D. Nghiem, "Liquid desiccant lithium chloride regeneration by membrane distillation for air conditioning," *Sep. Purif. Technol.*, vol. 177, pp. 121–128, 2017, doi: 10.1016/j.seppur.2016.12.031.

[50] Y. Guo, Z. Ma, A. Al-Jubainawi, P. Cooper, and L. D. Nghiem, "Using electrodialysis for regeneration of aqueous lithium chloride solution in liquid desiccant air conditioning systems," *Energy Build.*, vol. 116, pp. 285–295, 2016, doi: 10.1016/j.enbuild.2016.01.014.

[51] T. Wen, Y. Luo, M. Wang, and X. She, "Comparative study on the liquid desiccant dehumidification performance of lithium chloride and potassium formate," *Renew. Energy*, vol. 167, pp. 841–852, 2021, doi: 10.1016/j.renene.2020.11.157.

[52] N. M. B. Mohd zamri Abdullah, Suzana Yusup, "Synthesis and Dehumidification Performance of Calcium Chloride Derived from the Waste Shells of Anadara granosa," *Applied Mechanics and Materials (Volume 625)*, 2014. .

[53] M. Bhowmik, R. Anandalakshmi, and P. Muthukumar, "Numerical investigation of performance trade-off characteristics of a packed bed dehumidifier using aqueous blends of lithium chloride and calcium chloride," *Heat Mass Transf. und Stoffuebertragung*, vol. 56, no. 11, pp. 3093–3109, 2020, doi: 10.1007/s00231-020-02893-y.

[54] L. Weng, W. Song, D. J. Jacobs, and G. D. Elliott, "Molecular insights into water vapor absorption by aqueous lithium bromide and lithium bromide/sodium formate solutions," *Appl. Therm. Eng.*, vol. 102, pp. 125–133, 2016, doi: 10.1016/j.applthermaleng.2016.03.153.

[55] A. Xu *et al.*, "Performance analysis of a cascade lithium bromide absorption refrigeration/dehumidification process driven by low-grade waste heat for hot summer and

cold winter climate area in China," *Energy Convers. Manag.*, vol. 228, no. November 2020, p. 113664, 2021, doi: 10.1016/j.enconman.2020.113664.

[56] A. De Lucas, M. Donate, and J. F. Rodríguez, "Applying surfactants to improve the absorption capacity of mixtures of lithium bromide and formates in absorption refrigeration coolers," *Int. J. Refrig.*, vol. 31, no. 6, pp. 1073–1080, 2008, doi: 10.1016/j.ijrefrig.2007.12.005.

[57] A. Fakharnezhad and P. Keshavarz, "Experimental investigation of gas dehumidification by tri-ethylene glycol in hollow fiber membrane contactors," *J. Ind. Eng. Chem.*, vol. 34, pp. 390–396, 2016, doi: 10.1016/j.jiec.2015.12.021.

[58] G. Fekadu and S. Subudhi, "Renewable energy for liquid desiccants air conditioning system : A review," *Renew. Sustain. Energy Rev.*, vol. 93, no. April, pp. 364–379, 2018, doi: 10.1016/j.rser.2018.05.016.

[59] S. Jain and P. K. Bansal, "Performance analysis of liquid desiccant dehumidification systems," *Int. J. Refrig.*, vol. 30, no. 5, pp. 861–872, 2007, doi: 10.1016/j.ijrefrig.2006.11.013.

[60] M. Sahlot and S. B. Riffat, "Desiccant cooling systems: A review," *Int. J. Low-Carbon Technol.*, vol. 11, no. 4, pp. 489–505, 2016, doi: 10.1093/ijlct/ctv032.

[61] A. H. Abdel-Salam and C. J. Simonson, "State-of-the-art in liquid desiccant air conditioning equipment and systems," *Renew. Sustain. Energy Rev.*, vol. 58, pp. 1152–1183, 2016, doi: 10.1016/j.rser.2015.12.042.

[62] K. Landymore, "Electrical Energy Reduction in Refrigeration and Air," *Renew. Sustain. Energy Rev.*, vol. 80, p. 6, [Online]. Available: http://www.smartcool.net/documents/technology/White_Paper.pdf.

[63] Mohammad Afshin, "Selection of the Liquid Desiccant in a Run-Around Membrane Energy Exchanger," Saskatoon, 2010.

[64] S. Pintaldi, C. Perfumo, S. Sethuvenkatraman, S. White, and G. Rosengarten, "A review of thermal energy storage technologies and control approaches for solar cooling," *Renew. Sustain. Energy Rev.*, vol. 41, no. 1, pp. 975–995, 2015, doi: 10.1016/j.rser.2014.08.062.

[65]   E. Elsarrag, O. N. Igobo, Y. Alhorr, and P. A. Davies, "Solar pond powered liquid desiccant evaporative cooling," *Renew. Sustain. Energy Rev.*, vol. 58, pp. 124–140, 2016, doi: 10.1016/j.rser.2015.12.053.

[66]   R. Song, T. Zou, J. Chen, X. Hou, and X. Han, "Study on the Physical Properties of LiCl Solution," *IOP Conf. Ser. Mater. Sci. Eng.*, vol. 562, no. 1, 2019, doi: 10.1088/1757-899X/562/1/012102.

[67]   I. P. Koronaki, R. I. Christodoulaki, V. D. Papaefthimiou, and E. D. Rogdakis, "Thermodynamic analysis of a counter flow adiabatic dehumidifier with different liquid desiccant materials," *Appl. Therm. Eng.*, vol. 50, no. 1, pp. 361–373, 2013, doi: 10.1016/j.applthermaleng.2012.06.043.

[68]   M. Bhowmik, P. Muthukumar, and R. Anandalakshmi, "Experimental study of coupled heat and mass transfer phenomena between air and desiccant in a solar assisted thermal liquid desiccant system," *Int. J. Therm. Sci.*, vol. 162, no. July 2020, p. 106795, 2021, doi: 10.1016/j.ijthermalsci.2020.106795.